Current Biology 24, 1854–1865, August 18, 2014 ©2014 Elsevier Ltd All rights reserved http://dx.doi.org/10.1016/j.cub.2014.07.014

Article

PINK1 Triggers Autocatalytic Activation of Parkin to Specify Cell Fate Decisions

Conggang Zhang,[1] Schuyler Lee,[1] Yinghua Peng,[1] Eric Bunker,[1] Emilie Giaime,[2] Jie Shen,[2] Zongyao Zhou,[1] and Xuedong Liu[1,*]

[1]Department of Chemistry and Biochemistry, 3415 Colorado Avenue, Jennie Smoly Caruthers Biotechnology Building, University of Colorado Boulder, Boulder, CO 80303, USA

[2]Center for Neurologic Diseases, Brigham and Women's Hospital, Program in Neuroscience, Harvard Medical School, New Research Building, Room 636E, 77 Avenue Louis Pasteur, Boston, MA 02115, USA

Summary

Background: The PINK1-Parkin pathway is known to play important roles in regulating mitochondria dynamics, motility, and quality control. Activation of this pathway can be triggered by a variety of cellular stress signals that cause mitochondrial damage. How this pathway senses different levels of mitochondrial damage and mediates cell fate decisions accordingly is incompletely understood.

Results: Here, we present evidence that PINK1-Parkin has both cytoprotective and proapoptotic functions. PINK1-Parkin operates as a molecular switch to dictate cell fate decisions in response to different cellular stressors. Cells exposed to severe and irreparable mitochondrial damage agents such as valinomycin can undergo PINK1-Parkin-dependent apoptosis. The proapoptotic response elicited by valinomycin is associated with the degradation of Mcl-1. PINK1 directly phosphorylates Parkin at Ser65 of its Ubl domain and triggers activation of its E3 ligase activity through an autocatalytic mechanism that amplifies its E3 ligase activity toward Mcl-1.

Conclusions: Autocatalytic activation of Parkin bolsters its accumulation on mitochondria and apoptotic response to valinomycin. Our results suggest that PINK1-Parkin constitutes a damage-gated molecular switch that governs cellular-context-specific cell fate decisions in response to variable stress stimuli.

Introduction

Mutations in PINK1 and Parkin are associated with early-onset familial autosomal recessive Parkinson's disease (PD) [1, 2]. Although the exact molecular mechanism that causes PD is not clearly understood, genetic studies in model organisms coupled with mechanistic studies in mammalian cells suggest that PINK1 acts upstream of Parkin to regulate mitochondrial integrity, dynamics, and motility [3–5].

The level of PINK1 is low in unperturbed mitochondria due to proteolytic degradation of PINK1 by the protease ParL and subsequent retrotranslocation into the cytosol for proteasomal degradation [6]. Upon the loss of mitochondrial membrane potential by decouplers, such as cyanide, the import and degradation of PINK1 are blocked, allowing it to accumulate on the outer mitochondrial membrane [7–9]. Increased expression and activity of PINK1 lead to phosphorylation of mitofusin 2 [10], Parkin [9, 11], Miro [12], and other substrates. Elevated PINK1 activity promotes translocation of Parkin from the cytosol to the mitochondria. In accordance with the significance of Parkin mitochondrial recruitment, many patient-derived Parkin mutants are defective in mitochondrial translocation [13, 14]. Parkin is a member of the RING-IBR-RING (RBR) family of ubiquitin E3 ligases with a conserved catalytic cysteine residue analogous to the HECT domain E3s [15]. The autoubiquitination activity of Parkin is abolished if this residue is mutated [16, 17]. A diverse set of protein substrates have been shown be ubiquitinated by Parkin [2], including several proteins localized in the mitochondrial outer membrane, such as Mfn1 and Mfn2 [10, 18, 19], Drp1 [20], voltage-dependent anion channel 1 (VDAC1) [21], and Miro [12]. Ubiquitination and degradation of these proteins is linked to mitochondrial fission during mitophagy or mitochondrial motility. Proteomics studies revealed that Parkin may directly or indirectly regulate ubiquitination of more than 100 mitochondrial proteins upon mitochondrial depolarization [22].

Despite these current insights, there are still many outstanding questions that remain to be answered. First, the mechanism by which PINK1 mediates Parkin mitochondrial translocation is still incompletely understood. Second, it remains to be determined how the E3 ligase activity of Parkin is regulated. Biochemical and structure studies revealed that Parkin exists in an autoinhibited conformation due to an interaction between the N-terminal ubiquitin-like (Ubl) domain, the repressor element (REP), and the RING1 domain [23]. These observations raise an interesting question about the potential mechanisms that can allosterically activate Parkin in vitro and in vivo. Finally, the diversity of Parkin substrates begs the question whether there is selective ubiquitination of these substrates and whether ubiquitination of these substrates contribute to cell fate decisions in response to distinct cellular stress stimuli.

The PINK1-Parkin pathway has also been shown to have cytoprotective activity under various stress conditions [2, 5]. There appears to be distinct Parkin-dependent pathways for preventing cell death depending on the severity of mitochondrial damage and the nature of stress signals. Reactive oxygen species (ROS) can induce PINK1-Parkin-dependent repairing damaged mitochondria through the mitochondria-derived vesicle trafficking pathway [24]. Upregulation of Parkin-dependent NF-κB signaling has a prosurvival role under moderate stress [25]. Mitophagy is the best characterized PINK1-Parkin-dependent pathway for removal of damaged mitochondria [4]. Collectively, these results suggest that the PINK1-Parkin nexus can mount different cellular responses depending on the levels of cell stress signals.

Here, we investigated mechanisms by which PINK1-Parkin regulates cell survival. We discovered that beyond its well-recognized cytoprotective function, PINK1-Parkin is also required for valinomycin-induced apoptosis. Mechanistically, the proapoptotic function of PINK1-Parkin in response to severe apoptotic signal is associated with ubiquitination of the antiapoptotic protein Mcl-1 and activation of the caspase cascade. We reconstituted Parkin-dependent ubiquitination

*Correspondence: xuedong.liu@colorado.edu

of Mcl-1 in vitro and demonstrated that PINK1 allosterically regulates the Parkin E3 ligase activity through phosphorylation of Ser65 of Parkin. This phosphorylation event sets off autocatalytic activation of Parkin. Finally, our study showed that ubiquitin is also a substrate for PINK1 and phosphorylated ubiquitin promotes Parkin mitochondrial targeting and afford additional elevation of Parkin activity. Our results reveal a new function of the PINK1-Parkin pathway in cell fate decisions and a Parkin activation cascade in response to diverse stress stimuli.

Results

Parkin-Dependent Mitophagy and Apoptotic Cellular Responses in Response to Mitochondrial Depolarization

It is well established that the PINK1-Parkin pathway is involved in elimination of depolarized mitochondria by mitophagy [26]. As expected, HeLa cells stably expressing fluorescence protein tagged wild-type Parkin, but not mutant Parkin T240R (seen in Parkinson's patients), undergo mitophagy in the presence of the mitochondrial uncoupler protonophore carbonyl cyanide m-chlorophenyl hydrazone (CCCP) (Figure 1A). The mitophagic response can be demonstrated by the increased colocalization of Parkin and LC3 with the mitochondria marker RFP-Smac-mts (RFP-Smac)—a fusion of the mitochondrial targeting sequence of Smac with RFP (Figures S1A and S1 and Movies S1 and S2 available online). Under these conditions, no significant apoptosis is seen in either cell line based on RFP-Smac release (Figure 1B).

To further probe specificity of Parkin-induced mitophagy in response to mitochondrial depolarization, we tested mitophagic responses to a panel of mitochondrial damaging agents, including rotenone, dinitrophenol, and valinomycin. Surprisingly, we found only valinomycin, a potassium ionophore known to collapse the potassium gradient across the mitochondrial inner membrane and depolarize mitochondria, induces rapid cellular apoptosis in HeLa cells expressing wild-type Parkin, but not Parkin T240R mutant (Figures 1C and 1D and Movie S3). Valinomycin resistance is not due to the expression of the Parkin mutant since wild-type HeLa cells display identical apoptosis phenotype upon valinomycin treatment (data not shown). Valinomycin-induced cell death can be suppressed by treatment with the caspase inhibitor Z-VAD-FMK, which is consistent with cell death by apoptosis (Figures S1G and S1H). Both CCCP and valinomycin induce rapid Venus-Parkin accumulation on mitochondria with similar kinetics (Figures S1C–S1F). However, despite similar effects on Parkin mitochondrial accumulation, cells exposed to these two depolarizing agents adopt different cell fates.

PINK1 Is Required for Valinomycin-Induced Parkin-Dependent Apoptosis

Because Parkin-dependent mitophagy requires PINK1 stabilization and accumulation on mitochondria [7, 9, 13, 21], we investigated whether PINK1 is also required for Parkin-dependent apoptosis in response to valinomycin via small interfering RNA (siRNA)-mediated silencing of PINK1. Similar to what we observed for CCCP, valinomycin stabilized PINK1 expression (Figure 1F). As expected, PINK1 knockdown blocks Venus-Parkin accumulation on mitochondria and stabilization of PINK1 (Figures 1E and 1F). The levels of apoptosis are significantly reduced in PINK1 knockdown cells (Figures 1E–1G). This result indicates that the PINK1-Parkin pathway is involved in both mitophagy and apoptosis in response to the two different stimuli.

Valinomycin Specifically Suppresses the Expression of Antiapoptotic Protein Mcl-1 and Activates Initiator Caspase-8 and Caspase-9

To address the mechanism of valinomycin-induced apoptosis, we initially assessed the expression of antiapoptotic proteins and the activation status of several apoptotic hallmark proteins in Parkin wild-type and Parkin T240R mutant HeLa cells (Figure 2A). Expression of Parkin T240R is higher than that of wild-type Parkin, which may be a result of their differential stability in cells. However, this difference is unlikely to be important for interpreting the experimental results since Parkin T240R is effectively null in valinomycin-induced apoptotic responses and serves a better control to demonstrate the specificity of PINK1- and Parkin-dependent cellular responses. Interestingly, in cells expressing wild-type Parkin, valinomycin treatment slightly elevated PINK1 expression at 2 hr, after which levels declined and suppressed. In contrast, valinomycin strongly induced expression of PINK1 in HeLa cells expressing Parkin T240R mutant (Figure 2A, top panel). The pattern of PINK1 induction in the absence of functional Parkin in HeLa cells is reminiscent to CCCP treatment described previously [26]. Among the three well-characterized Bcl2 proteins, only Mcl-1 is significantly downregulated by valinomycin treatment in a Parkin-dependent manner. No changes in Bcl-xL or Bcl2 were observed. Valinomycin treatment causes activation of initiator caspase-8 and caspase-9 within 4 hr in HeLa cells expressing wild-type Parkin, but not in cells expressing mutant Parkin (Figure 2A). In agreement with strong apoptotic activation by valinomycin, effector caspase-3, caspase-7, and PARP are cleaved in a Parkin-dependent manner (Figure 2A). To determine whether suppression of Mcl-1 is due to Parkin-dependent ubiquitin-mediated degradation, we treated HeLa cells with or without Parkin expression with valinomycin in the presence or absence of the proteasome inhibitor MG132. High-molecular-weight Mcl-1 only presents in cells expressing Parkin and accumulates in the presence of MG132 (Figure 2B, lane 8). This finding suggests that Mcl-1 is most likely ubiquitinated by Parkin upon treatment with valinomycin. Activation of apoptosis by valinomycin is associated with suppression of Mcl-1 and activation of the intrinsic and extrinsic apoptotic initiator caspases.

If Mcl-1 suppression is linked to differences in cell fate upon exposure to CCCP and valinomycin, we would expect that CCCP should not cause significant Mcl-1 degradation. Immunoblotting analysis revealed that CCCP only causes a slight drop in Mcl-1 and remains stabilized after 6 hr, as opposed to the steady decline of Mcl-1 in response to valinomycin (Figures 2C and 2D). Conversely, if Mcl-1 level is a key determinant of cell fate decision, reduction of Mcl-1 should be sufficient to alter the CCCP response. To test this hypothesis, we knocked down expression of Mcl-1 by small hairpin RNA (shRNA; Figure 2E). As shown in Figure 2F, HeLa cells with lower endogenous Mcl-1 undergo apoptosis in response to CCCP. These data suggest that Parkin catalyzes selective degradation of specific substrates in response to specific stimuli. Suppression of Mcl-1 by Parkin is critical for differential cell fate decisions in response to CCCP and valinomycin.

Valinomycin Induces PINK1- and Parkin-Dependent Apoptotic Response in MEFs

To determine whether the endogenous PINK1 or Parkin is required for valinomycin-induced apoptosis in another cell system, we first investigated the response to valinomycin in mouse embryonic fibroblasts (MEFs) derived from the parental and PINK1-knockout mice, as well as in MEFs from

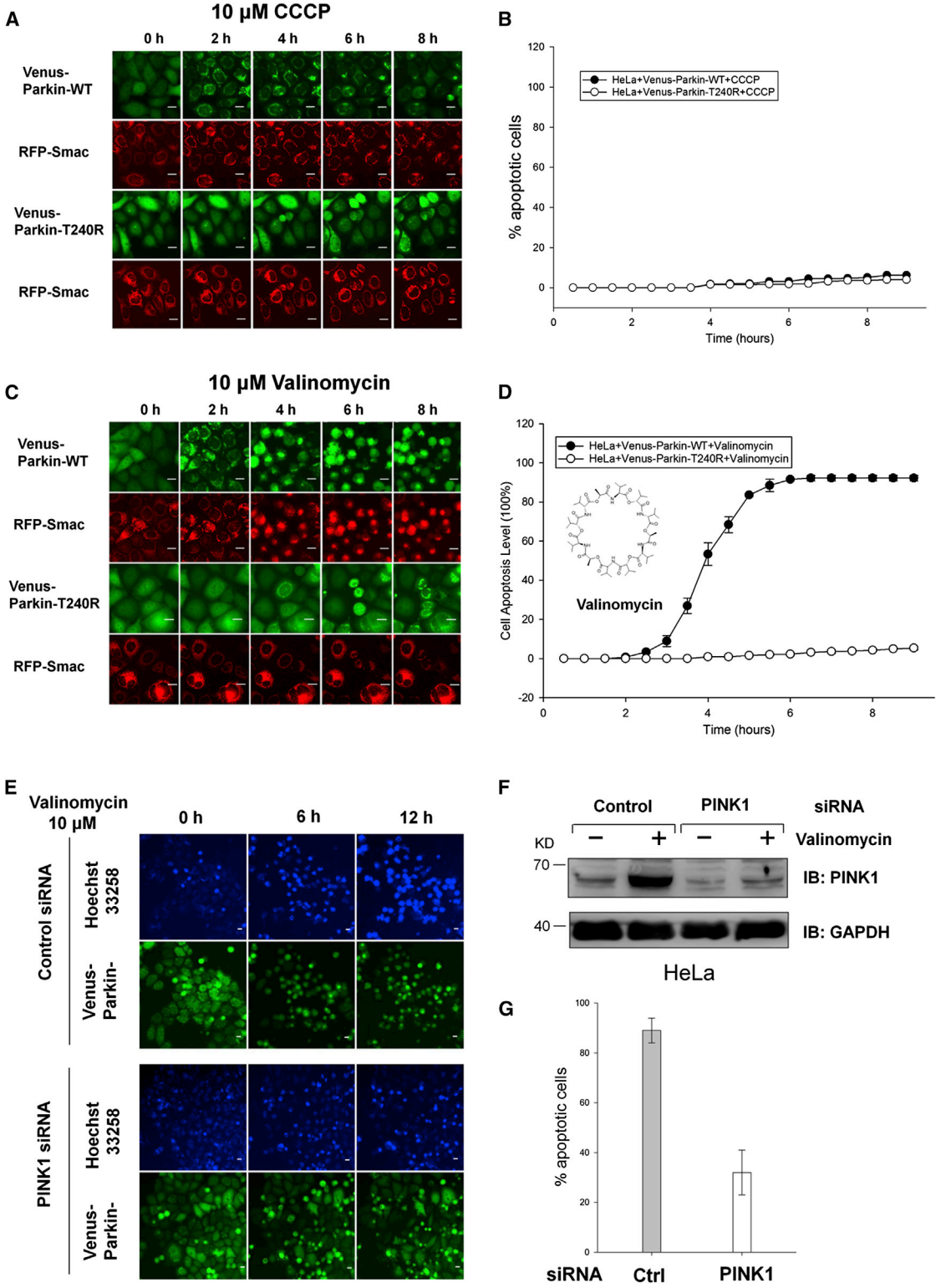

Figure 1. Valinomycin Triggers Parkin Mitochondrial Recruitment and Apoptosis in a PINK1- and Parkin-Dependent Manner

(A–D) HeLa cells expressing RFP-Smac-mts and either Venus-Parkin-WT or Venus-Parkin-T240R were treated with 10 μM CCCP (A and B) or 10 μM Valinomycin (C and D) in a 9 hr time course. Scale bars, 10 μm.

(A) CCCP induced mitochondrial recruitment of Parkin-WT, but not Parkin-T240R. Neither Parkin-WT nor Parkin-T240R triggered RFP-Smac release from the mitochondria.

(B) Apoptotic cell death was quantified by counting of cells positive for RFP-Smac release. CCCP did not trigger significant RFP-Smac release in either cell line.

(C) Valinomycin induced mitochondrial recruitment of Parkin-WT, but not Parkin-T240R.

(legend continued on next page)

Parkin-knockout mice [27]. Using time-lapse live-cell imaging, we monitored cell apoptotic responses during the time course of valinomycin exposure by a caspase-3 activity sensor, NucView 488 (Biotium). DEVD-NucView 488 caspase-3 substrate is a cell-membrane-permeable fluorescence sensor. Upon cleavage by active caspase-3, the DNA-binding dye is released and migrates to the cell nucleus to stain the nucleus bright green. The nuclei and their condensation states were also scored independently by Hoechst 33258 fluorescence using an automated MetaXpress application module. As seen in HeLa cells, parental wild-type MEFs are more prone to valinomycin-induced apoptosis than are PINK1- or Parkin-null MEFs (Figures 3A and 3B). To further demonstrate that the endogenous PINK1 has a proapoptotic role in valinomycin-induced apoptotic response, we knocked down the expression of PINK1 in wild-type MEFs using shRNA. A mammalian nontargeting (NT) shRNA was used as a control. Depletion of PINK1 was confirmed by immunoblotting (Figure 3C). Treatment with valinomycin-induced stronger apoptosis in control MEFs (Figures 3C and 3D). Treatment with valinomycin also suppressed Mcl-1 expression in the control MEFs (Figure 3E). However, downregulation of Mcl-1 was partially abrogated in PINK1 knockdown MEFs (Figure 3E). These results suggest that valinomycin induces PINK1- and Parkin-dependent suppression of Mcl-1 and apoptosis in MEFs.

We tested whether valinomycin sensitivity can be rescued in PINK1- or Parkin-null MEFs by stably expressing the two genes. The human versions of these genes were used because commercial antibodies against mouse Parkin are largely ineffective. Nevertheless, stable expression of human PINK1 and Parkin fully restores the defects of valinomycin response in MEFs that are deficient for either gene (Figures 3A and 3B). Immunoblotting confirmed a similar pattern of regulation of caspases and Bcl2 proteins as that seen in HeLa cells (Figure S2A), as well as Z-VAD-FMK sensitivity (Figures S2B and S2C). These findings indicate that the PINK1-Parkin pathway controls cell fate determination in response to valinomycin.

PINK1 Phosphorylates a Highly Conserved Ser65 Residue in the Parkin Ubl Domain and Ubiquitin

To further probe the biochemical mechanisms by which PINK1 and Parkin regulate cellular apoptosis, we investigated how the PINK1 and Parkin activity controls Mcl-1 ubiquitination in vitro. Our initial attempt was to use recombinant PINK1 to drive the pathway. Despite intensive efforts, we were unable to detect robust kinase activity of human PINK1. Previous studies by Muqit and colleagues showed that an insect ortholog of PINK1 (TcPINK1) from *Tribolium castaneum* is catalytically active [28]. In agreement with the previous report, we find that TcPINK1 can phosphorylate human Parkin$^{1–108}$ and that Ser65 is most likely the site targeted by TcPINK1 as no phosphorylation can be detected when Ser65 was mutated to Ala (Figure 4A, lane 1 versus lane 2). Despite robust phosphorylation of recombinant human Parkin$^{1–108}$ by TcPINK1 in vitro, full-length human Parkin was reported to be a poor substrate for TcPINK1 [11]. In light of the recent success with the full-length rat Parkin (rParkin) protein in structural studies [23], we tested whether recombinant rParkin may be a better substrate for TcPINK1 because rParkin is well folded. As shown in Figure 4B, rParkin is robustly phosphorylated by TcPINK1. Mutation of catalytic Cys at 431 to Ser does not affect its phosphorylation. However, mutation of Ser65 to Ala in the Ubl domain of rParkin largely eliminates its phosphorylation (Figure 4B, lanes 7–9). Since the Ubl domain of Parkin shares significant sequence and structure homology with ubiquitin and Ser65 is conserved and solvent exposed (Figures S3A–S3C), we tested whether ubiquitin may also be a substrate for PINK1. As seen with Parkin Ubl, TcPINK1 can phosphorylate wild-type ubiquitin and this phosphorylation is significantly reduced when Ser at 65 is mutated to Ala or Asp (Figure S4A), suggesting that Ser65 is the primary phosphorylation site of ubiquitin. These results indicate that PINK1 phosphorylates Parkin and ubiquitin primarily at a single Ser residue (Ser65).

Mcl-1 Is a Substrate for Parkin E3 Ubiquitin Ligase

To demonstrate that Mcl-1 is a substrate for Parkin, we reconstituted Parkin-dependent Mcl-1 ubiquitination using highly purified ubiquitin, Uba1(E1), UbcH7 (E2), rParkin, and Mcl-1 (Figure 4C). The mixture was incubated for 3 hr at room temperature (Figure 4D). Polyubiquitination of Mcl-1 is more robust with a Parkin^{W403A} (Figure 4D, lane 7 versus lane 8), a mutant that has been shown to inactivate the REP element and to elevate its autoubiquitination activity [23]. A double mutant with the substitution of catalytic Cys 431 to Ser has no activity (Figure 4D, lane 9). Omission of any component required in the ubiquitin transfer reaction abrogated polyubiquitination of Mcl-1, suggesting this reaction is highly specific (Figure 4D, lanes 1–6). This finding indicates Mcl-1 is a substrate for Parkin in vitro.

Activation of Parkin E3 Ubiquitin Ligase Activity by PINK1 through Phosphorylation of Parkin Ubl at Ser65

Given that Parkin Ser65 is phosphorylated by PINK1, we analyzed the effects of Parkin phosphorylation on its autoubiquitination and Mcl-1 ubiquitination activity. As shown in Figure 4E, GST-rParkin is phosphorylated by PINK1, and this phosphorylation is absent in GST-rParkin^{S65A}, as detected by a Parkin phospho-Ser65 antibody (Figure 4E, lane 2 versus lane 3). Phosphorylation of Parkin greatly increases its auto- and transubiquitination activity by the early appearance of high-molecular-weight Parkin conjugates and ubiquitinated Mcl-1 (Figure 4E, lanes 5 and 6 versus lanes 7 and 8). GST-rParkin^{S65A} is inactive in the presence or absence of PINK1 (Figure 4E, lanes 3 and 4 versus 9 and 10). Since PINK1 also phosphorylates ubiquitin at Ser65 (Figure S4A), we also tested the effect of this phosphorylation on Parkin E3 ligase activity. Ubiquitin was first incubated with PINK1 or kinase-dead PINK1 for 2 hr to allow it to be phosphorylated. Phosphorylated ubiquitin and control ubiquitin were used as inputs in the reconstituted Mcl-1 ubiquitination reaction by Parkin

(D) Quantitation of cell death by counting of cells positive for RFP-Smac release in valinomycin-treated cells.
(E–G) HeLa cells expressing Venus-Parkin-WT were transfected with control or PINK1 siRNA and were treated with 10 μM valinomycin in a 12 hr time course. Apoptotic cell death was visualized by staining with Hoechst 33258, which enters all cells regardless cell health. The average intensity of DNA labeling significantly increases in apoptotic cells as nuclei condense during apoptosis. Quantitation of cell death was performed using the automated cell heath application module in MetaXpress software. Representative images are shown. Scale bars, 10 μm.
(E) PINK1-dependent apoptotic cell death was visualized by fluorescent microscopy. Cells were incubated with valinomycin for 1.5h prior to image capture.
(F) Wild-type and PINK1 knockdown cells in response to valinomycin were immunoblotted using an antibody for PINK1.
(G) Apoptotic cell death was quantified by counting of cells positive for cells with condensed chromatin at 12h. More than 500 cells were scored.
Error bars represent the SD. See also Figure S1 and Movies S1, S2, and S3.

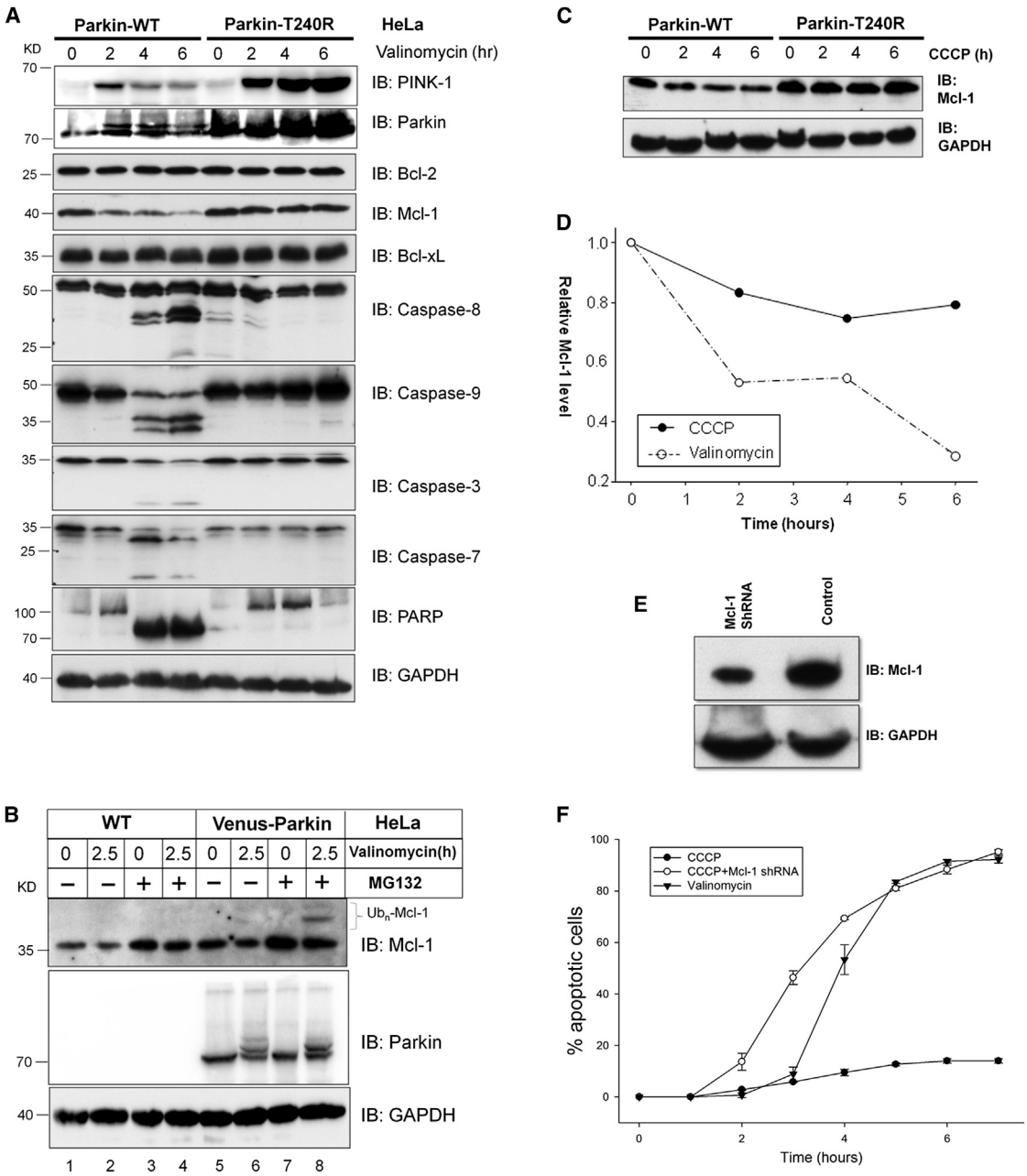

Figure 2. Valinomycin Induces Parkin-Dependent Suppression of Mcl-1 and Activation of Apoptotic Initiator Caspases

(A) HeLa cells expressing Parkin-WT or Parkin-T240R were subjected to 10 μM valinomycin in a 6 hr time course and were collected at 2 hr intervals. Proapoptotic and antiapoptotic proteins were monitored by western blotting using antibodies for their respective proteins. Upon valinomycin treatment, cells expressing Parkin-WT exhibited a depletion of Mcl-1 levels, activation of caspase-8 and caspase-9, and cleavage of caspase-3, caspase-7, and PARP. The corresponding apoptotic response was not detected in cells expressing Parkin-T240R.

(B) HeLa cells with or without Parkin expression were treated with 10 μM valinomycin and/or 10 μM MG132 for 2.5 hr. The response was monitored by western blotting using an antibody for Mcl-1 and Parkin. Cells expressing Parkin degrade Mcl-1 when treated with valinomycin and accumulated Ub-Mcl-1 when treated simultaneously with the proteasome inhibitor MG132.

(C) Effect of CCCP on Mcl-1 levels. The indicated cell lines were treated with 10 μM CCCP in a 6 hr time course. Endogenous Mcl-1 was blotted with anti-Mcl-1 with GAPDH as a loading control.

(D) Mcl-1 levels from (A) and (C) were plotted.

(E) Suppression of endogenous Mcl-1 expression by shRNA. Stable knockdown HeLa cells expression Venus-Parkin and RFP-Smac were obtained by infection with shRNA for Mcl-1.

(F) CCCP induces apoptosis in HeLa cells with reduced Mcl-1 expression. Apoptotic cell death was quantified by counting of cells positive for RFP-Smac release. Error bars represent the SD.

See also Figure S2.

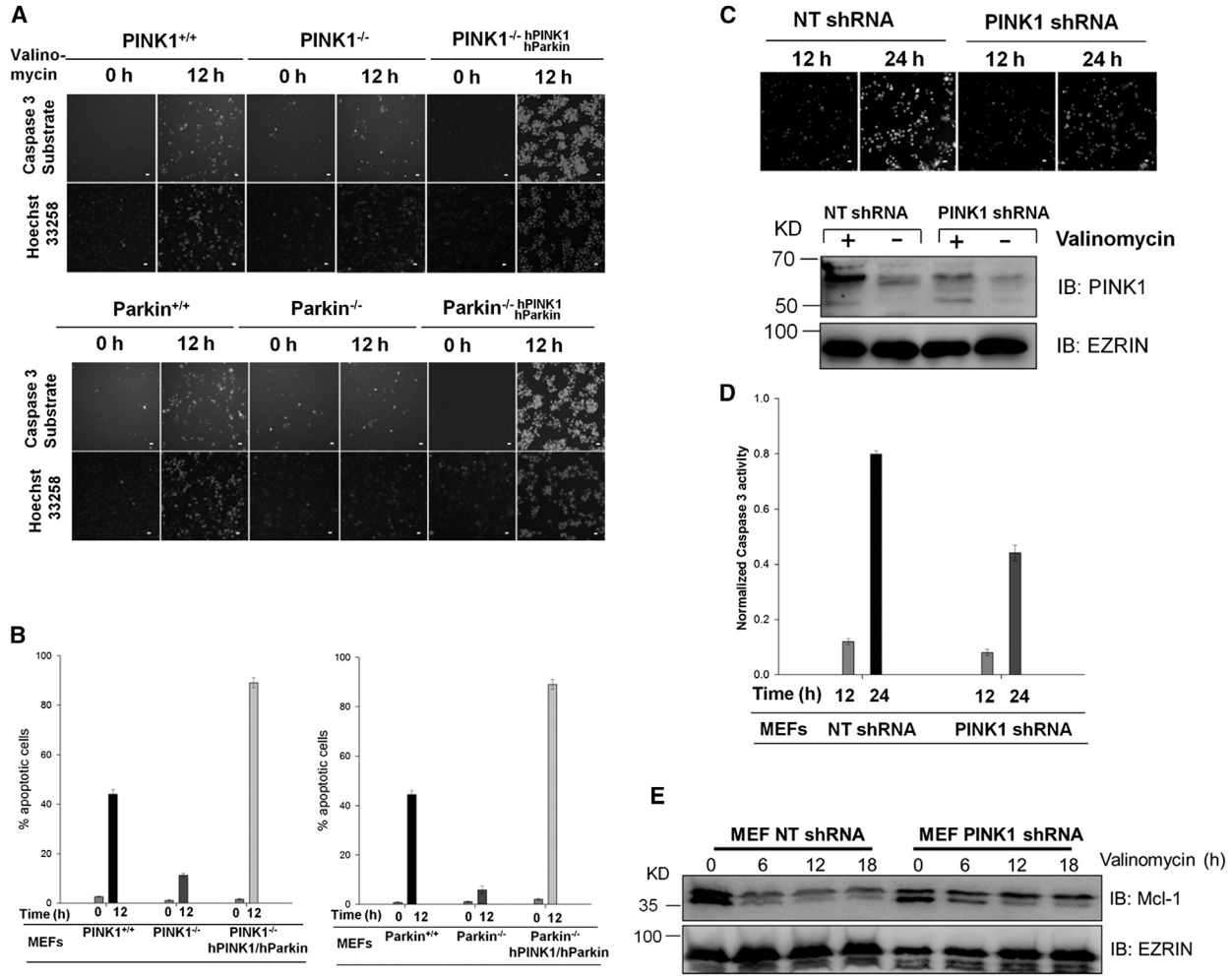

Figure 3. Valinomycin-Induced Apoptosis Requires PINK1 and Parkin

(A and B) Wild-type MEFs, PINK1- or Parkin-null MEFs, or MEF nulls reconstituted with human PINK1 and Parkin were stained with NucView caspase-3 sensor and Hoechst 33258 and treated with 10 μM valinomycin for 12 hr. Apoptotic cell death was visualized with fluorescent microscopy (A) and was quantified by measurement of the percentage of apoptotic nuclei (B). Scale bars, 10 μm.

(C) Wild-type MEFs were stably introduced with nontargeting or PINK1 shRNA and were treated with 10 μM valinomycin for 24 hr. PINK1 expression in control and knockdown cells was measured by western blotting. Apoptosis was monitored by caspase-3 sensor and quantified.

(D) PINK1 knockdown attenuates valinomycin-induced apoptosis as determined by caspase-3 activation.

(E) PINK1 knockdown relieves the suppression of Mcl-1 level by valinomycin.

Error bars represent the SD.

in vitro. In the reaction with phosphorylated ubiquitin, ubiquitinated Mcl-1 showed up earlier than the control reaction (Figure S4B, lanes 1–3 versus lanes 4–6) as well as the autoubiquitinated Parkin bands. Consistent with the positive effect of ubiquitin phosphorylation, phosphomimetic ubiquitin^{S65D} stimulates Parkin autoubiquitination more effectively than does ubiquitin^{S65A} with Ser65 phosphorylated rParkin or unphosphorylated rParkin (Figure S4C). These results indicate that phosphorylation of Parkin by PINK1 contributes to its activation in vitro. The effect of ubiquitin Ser65 phosphorylation on Parkin mitochondrial recruitment was tested by comparison of HA-Ub and HA-Ub^{S65A} in HeLa cells expressing Venus-Parkin. Expression of HA-Ub^{S65A}, but not HA-Ub, caused a significant reduction in Parkin recruitment to mitochondria in response to valinomycin treatment (Figures S4D and S4E). This result points to a potential role for ubiquitin phosphorylation in Parkin recruitment to mitochondria.

Phosphorylation of Parkin Ser65 Is Required for Valinomycin-Induced Apoptotic Responses

To address the significance of Parkin Ser65 phosphorylation in Parkin proapoptotic signaling in response to valinomycin, we stably expressed mTurquoise-Parkin^{S65A} in Parkin-null MEFs and HeLa cells. The mitochondrial recruitment behavior of mTurquoise-Parkin is identical to that of Venus-Parkin (data not shown). Whereas valinomycin induces wild-type Parkin mobility shift (Figure 5A), Parkin^{S65A} is largely unresponsive to valinomycin treatment. mTurquoise-Parkin^{S65A} is also defective in mitochondrial recruitment in response to valinomycin (Figures 5B and 5C). MEFs expressing mTurquoise-Parkin^{S65A} are resistant to valinomycin-induced cell death (Figures 5B and 5C), suggesting that phosphorylation of Parkin Ser65 is required for initiating Parkin recruitment to mitochondria and transducing apoptotic signal.

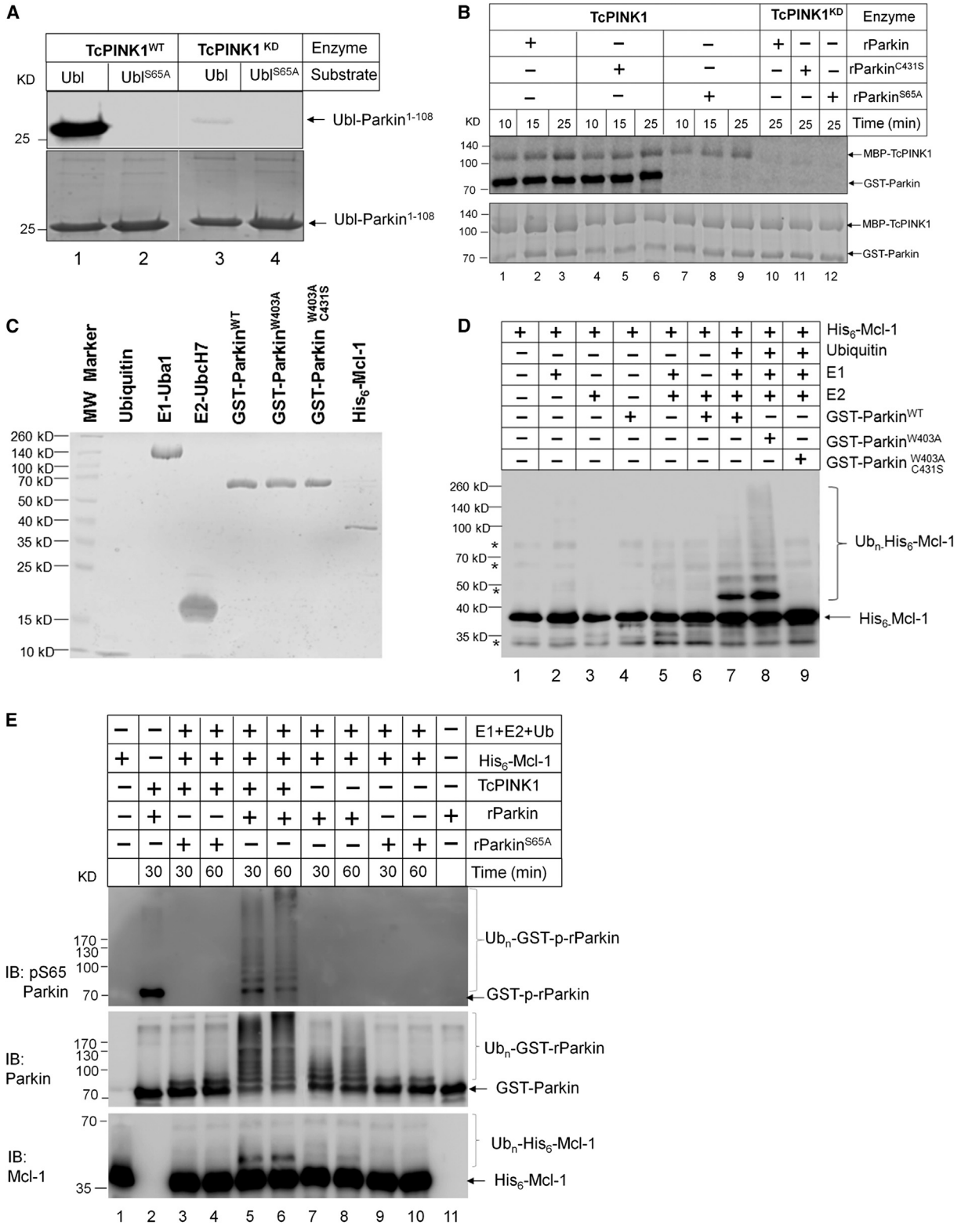

Figure 4. Full-Length Parkin and Parkin Ubl Domain Are PINK1 Substrates and In Vitro Reconstitution of Mcl-1 Ubiquitination by Parkin

(A and B) In vitro kinase assay with [γ-^{32}P] ATP.

(A) Ubl^{WT}-Parkin$^{1–108}$ or Ubl^{S65A} -Parkin$^{1–108}$ as the substrate for TcPINK1^{WT}. Ser65 in the Parkin Ubl domain is required for PINK1 phosphorylation.

(B) Phosphorylation of rParkin^{WT}, rParkin^{C431S}, or rParkin^{S65A} by TcPINK1^{WT} and kinase-dead TcPINK1^{D359A}.

(C) Coomassie blue staining of proteins used in the in vitro ubiquitination reaction.

(D) In vitro ubiquitination assay was performed at 37°C for 3 hr using 1 μM His$_6$-Mcl-1 as the substrate and was monitored by western blotting using an antibody for Mcl-1. rParkin-^{W403A} exhibiting enhanced autoubiquitination and rParkin^{W403AC431S} exhibiting no ligase activity were used as controls. rParkin (0.7 μM) was used in ubiquitination reactions.

(legend continued on next page)

Autocatalysis Is a Key Mechanism for Parkin Activation and Mitochondrial Recruitment

Inefficient accumulation of Parkin^{S65A} on mitochondria could be due to its inability to associate with mitochondria or to lack of catalytic activity to generate a positive feedback that is required for rapid and efficient activation of Parkin. Since Ser65 phosphorylated Parkin has robust autoubiquitination activity, we reasoned that the defect of Parkin^{S65A} in mitochondrial recruitment could be rescued by the presence of wild-type Parkin in *trans*. We tested this hypothesis by expressing Venus-Parkin and mTurquoise-Parkin^{S65A} independently or together in the same HeLa cells. As expected, Venus-Parkin is recruited to mitochondria, whereas mTurquoise-Parkin^{S65A} is not, when expressed independently upon valinomycin treatment (Figure 5D). In contrast, when both were coexpressed in the same cell, we found that mTurquoise-Parkin^{S65A} is efficiently recruited and indistinguishable from Venus-Parkin at 2 hr (Figures 5E and 5F). Detailed kinetics analysis revealed that there was an approximately 10 min delay in the early phase of accumulation for mTurquoise-Parkin^{S65A} and that both approached similar levels at approximately 110 min (Figure 5G). This result suggests that catalytically active Parkin converts Parkin^{S65A} to the wild-type Parkin phenotype in terms of mitochondrial recruitment.

One hypothesis that can explain the rescue of Parkin^{S65A} by wild-type Parkin is that Parkin activation is through an autocatalytic mechanism. To test this hypothesis, we set up an in vitro ubiquitination assay using a combination of wild-type and mutant Parkin proteins (Figures 6A and 6B). An untagged rParkin^{S65A} was purified to mix with either GST-rParkin or GST-rParkin^{S65A} at 3:1 ratio for the ubiquitination reaction after incubation with TcPINK1 to allow phosphorylation of GST-rParkin to occur. With a 3-fold reduction of GST-rParkin, the rate of Parkin autoubiquitination slowed down (Figure 6A, lanes 6–8 versus, Figure 4E, lanes 5 and 6). When non-phosphorylatable untagged rParkin^{S65A} was included in the reaction, polyubiquitination of rParkin^{S65A} occurred, judging by the disappearance of the substrate (Figure 6A, top panel, lanes 3–5). No reaction was seen in the control with GST- rParkin^{S65A} with rParkin^{S65A} (Figure 6A, lanes 9–11), suggesting that neither protein has catalytic activity in the presence of TcPINK1. With the Parkin pSer65 antibody, we can see that the autoubiquitination rate of GST-rParkin increased dramatically in the presence of rParkin^{S65A} (Figure 6A, lanes 3–5 versus lanes 6–8). This is unlikely to be due to the stimulation of GST-rParkin phosphorylation by rParkin^{S65A} since the overall phosphorylation of GST-rParkin stayed the same (Figure 6A, lanes 3–5). This result indicates that Parkin activation likely occurs via an autocatalytic mechanism. PINK1 phosphorylation of Parkin at Ser65 provides the initial spark for the nonlinear amplification of Parkin activity.

Autocatalytic Activity, but not Mitochondrial Recruitment, of Parkin Is Required for Parkin-Dependent Apoptotic Response to Valinomycin

Previous studies have shown that mitochondrial expression of linear ubiquitin chain promotes mitochondrial targeting of Parkin^{C431S} mutant that is defective in ubiquitin E3 ligase activity in response to CCCP [16]. To test whether mitochondrial recruitment of Parkin is sufficient for triggering apoptotic response in the presence of valinomycin, we stably expressed mitochondrial targeted linear ubiquitin chain Tom70-4xUbi in Parkin$^{-/-}$ MEFs along with Venus-Parkin^{C431S}. Immunoblotting showed that Parkin^{C431S} had an extra high-molecular-weight band, which was independent of valinomycin treatment or Tom70-4xUbi expression (Figures S5A and S5B). Upon treatment with valinomycin, Venus-Parkin^{C431S} accumulates on mitochondria in 40% of cells expressing both proteins, compared to less than 5% cells expressing Venus-Parkin^{C431S} alone at 90 min (Figures S5C and S5D). Meanwhile, valinomycin-induced apoptosis is indistinguishable between these two cell lines, similar to the cell line expressing Venus-Parkin^{S65A}, whereas Venus-Parkin showed dramatic apoptotic response (Figures S5E and S5F). Thus, in the absence of catalytic activity, Parkin recruitment to mitochondria does not switch cellular responses. This result suggests that Parkin mitochondrial targeting alone is insufficient to trigger valinomycin-induced apoptosis and is in line with the notion that Parkin autocatalytic activation and ubiquitination of Mcl-1 are required for mediating the apoptotic responses.

Discussion

Here we show that the PINK1-Parkin pathway can mediate different cell fates in response to different cell stress stimuli. We uncovered a new proapoptotic function of PINK1 and Parkin when cells are exposed to valinomycin in addition to its well-documented role in mitophagy and cytoprotection. The PINK1-Parkin-dependent apoptotic response is associated with suppression of Mcl-1. PINK1 phosphorylates Parkin at Ser65 and unleashes the autocatalytic activity of Parkin and ubiquitination of Mcl-1, which contributes to irreversible molecular switches that result in apoptotic responses. In addition, we reveal that PINK1 can also phosphorylate ubiquitin at Ser65. These two posttranslational events bolster Parkin accumulation on mitochondria and apoptotic response to valinomycin. Our results suggest that PINK1-Parkin constitutes a damage-gated molecular switch that governs cellular context-specific cell fate decisions in response to variable stress stimuli.

PINK1 as a Molecular Gauge for Cellular Stress

The antiapoptotic and cytoprotective function of PINK1 against cell stressors has been well recognized, although the exact mechanism is still debatable. For example, PINK1 is known to antagonize MG132-induced cell death [29–31]. The prosurvival function of PINK1 has been attributed to the inhibition of BAX translocation by cytoplasmic PINK1 activity [31] or phosphorylation of Bcl-xL by mitochondrial PINK1 [29, 30]. Some of the protective activity of PINK1 is independent of Parkin or its mitochondria recruitment as PINK1 without mitochondria targeting signal retains antiapoptotic activity in response to MG132 or MPTP [31, 32]. Here, we demonstrate that PINK1 can also mediate proapoptotic signals and that this function requires Parkin. To reconcile this apparent paradoxical role of PINK1 in cell death regulation, we have to consider

(E) Phosphorylation of Parkin Ser65 promotes Parkin auto- and transubiquitination activity. Wild-type rParkin and Ser65 rParkin mutant were incubated with TcPINK1 or kinase-dead TcPINK1 for 60 min prior to initiation of ubiquitination reactions. Phosphorylation of Ser65 of Parkin was monitored by a Ser65 phosphospecific antibody. Ubiquitin ligase activity was monitored by western blotting using an antibody for pSer65 Parkin, Parkin, and Mcl-1. Ubiquitination reactions were terminated at the indicated times.
See also Figures S3 and S4.

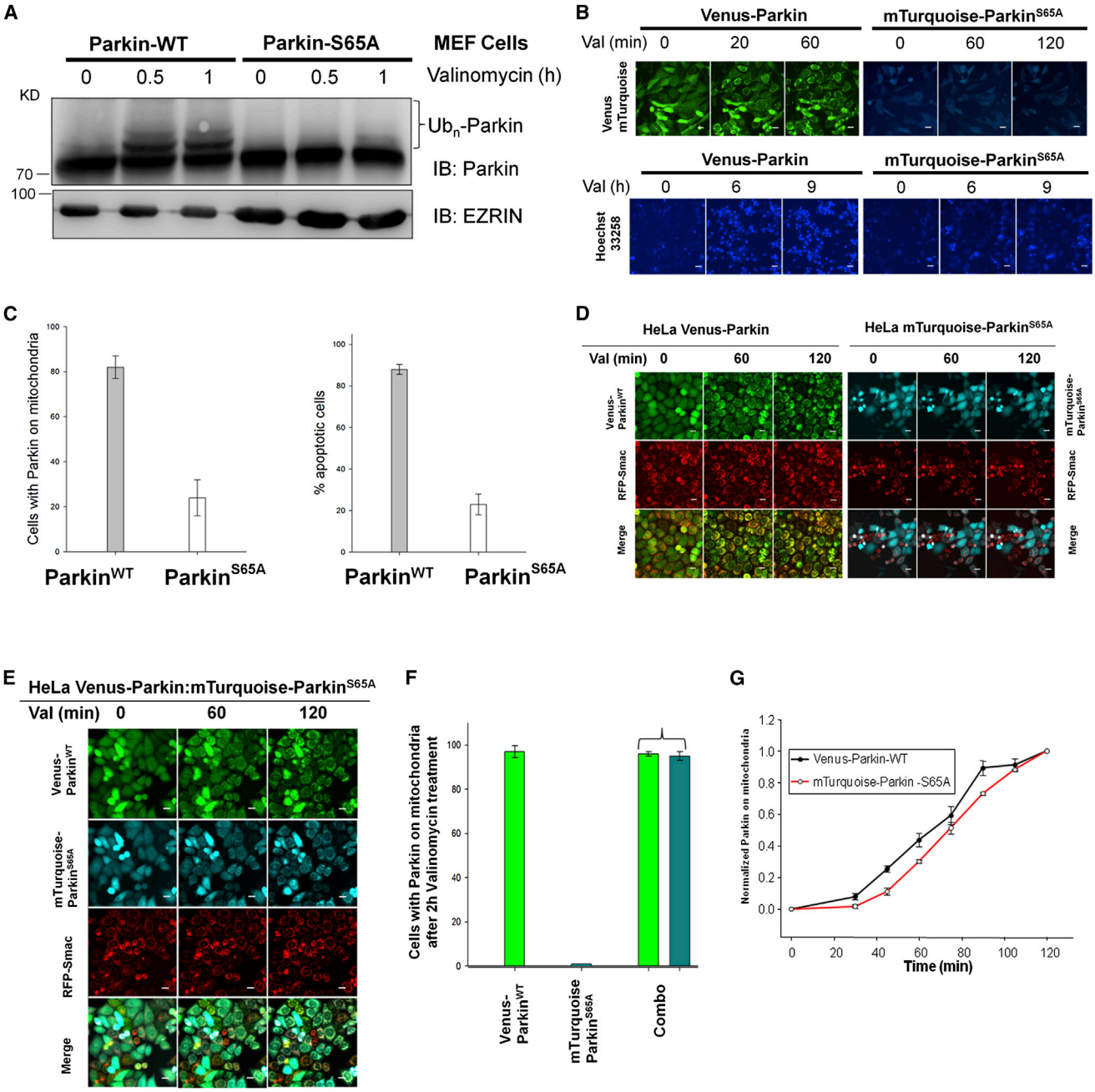

Figure 5. Phosphorylation of Parkin Ser65 Is Required for Valinomycin-Induced Apoptosis

PINK1$^{-/-}$ Parkin$^{-/-}$ MEF^{hPINK1} cells expressing Venus-Parkin or mTurqoise-Parkin^{S65A} were treated with valinomycin for the indicated times.

(A) Immunoblotting analysis of Parkin and Parkin^{S65A} response to valinomycin treatment.

(B) Parkin mitochondrial recruitment is perturbed by Ser65 mutation. Cells expressing mTurqoise-Parkin^{S65A} are resistance to valinomycin in apoptosis.

(C) Quantitation of (B).

(D and E) Parkin mitochondrial recruitment upon treatment with valinomycin in HeLa cells expressing either Venus-Parkin or mTurqoise-Parkin^{S65A} (D) or both Venus-Parkin and mTurqoise-Parkin^{S65A} (E). Scale bars, 10 μm.

(F) Quantitation of Venus-Parkin or mTurqoise-Parkin^{S65A} accumulation on mitochondria.

(G) Time course of Venus-Parkin and mTurqoise-Parkin^{S65A} mitochondrial recruitment in response to valinomycin treatment in double-positive HeLa cells. Error bars represent the SD. See also Figure S5.

the type of cellular damage each cellular stressor inflicts. McLelland et al. recently showed that excessive production of ROS by antimycin A causes mild oxidative damage, which generates mitochondria-derived vesicles in PINK1- and Parkin-dependent manner. These vesicles contain oxidized cargo that is transported to lysosomes for disposal [24] (Figure 7). This pathway is distinct from PINK1-Parkin-dependent mitophagy, which is triggered by the dissipation of $\Delta\psi m$ as a result of exposure to decouplers such as CCCP and irreversible damage of mitochondria. In many cellular contexts,

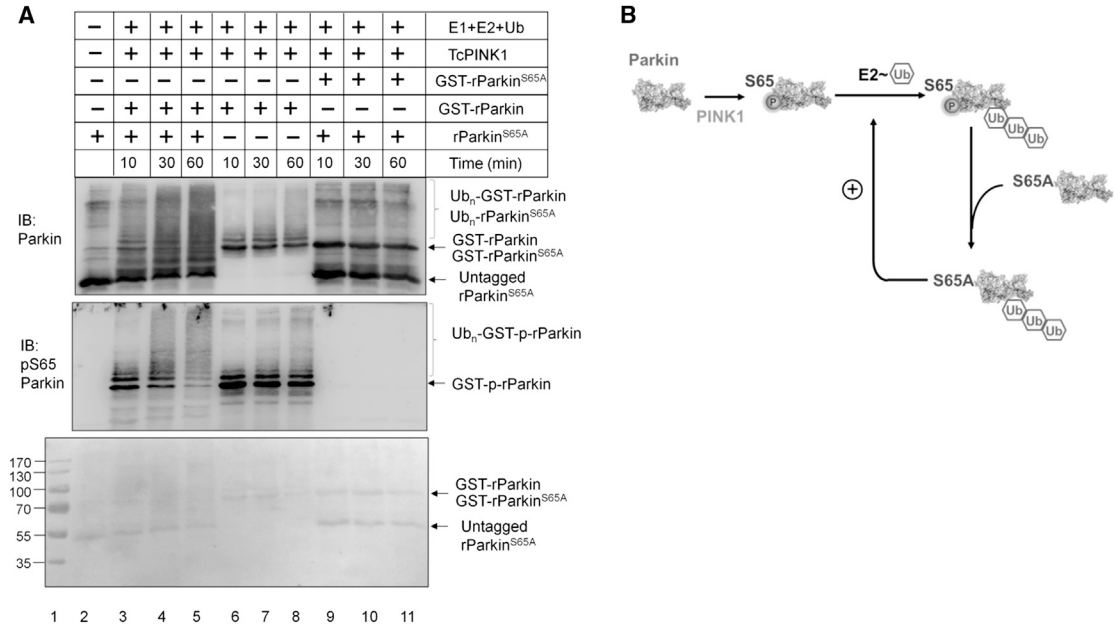

Figure 6. Autocatalytic activation of Parkin by PINK1

(A) In vitro ubiquitination of wild-type and mutant Parkin through autocatalysis. A total of 0.15 μM GST-rParkin or GST-rParkin^{S65A} was mixed with 0.45 μM rParkin^{S65A} prior to incubation with 0.5 μM TcPINK1 for phosphorylation at 30°C for 60 min. Ubiquitination reactions were monitored by immunoblotting with anti-Parkin or anti-pSer65 Parkin antibodies.

(B) Schematic diagram of the autocatalytic ubiquitination reaction.

mitophagy or autophagy may act as a rescue mechanism that the cell uses to escape from cell death [33]. With the treatment of valinomycin, the severity of mitochondria or organelle damage is most likely heightened to a threshold beyond repair due to severe stress. Under these conditions, the PINK1-Parkin pathway executes apoptotic program. Hence, the cell fate determination dictated by PINK1 or Parkin can be stimulus specific.

Stimuli Specific Degradation of Substrates by PINK1-Parkin Pathway

We found that valinomycin and CCCP treatment caused different cell fates via the same PINK1 and Parkin activation. The levels and kinetics of Parkin mitochondrial recruitment are comparable (Figure S1). This result suggests the cell fate decisions are AND gates since Parkin mitochondrial recruitment alone is insufficient. Indeed, we discovered that the endogenous Mcl-1 level set by Parkin recruitment followed by ubiquitination specifies mitophagy versus apoptosis decision in response to CCCP or valinomycin. Therefore, targeting of Parkin to mitochondria does not lead indiscriminate substrate ubiquitination. There are additional stimulus-specific changes that are in play. Our study identified a key determinant in Mcl-1 level and an AND gate in cell fate decisions. Future studies are needed to uncover stimuli specific determinant that makes Mcl-1 susceptible to Parkin ubiquitination. Regardless of the specificity factor of Mcl-1 degradation, our results suggest that PINK1-Parkin pathway serves as damage-gated molecular switch to specify distinct cell fate decisions (Figure 7).

An Autocatalytic Mechanism for the PINK1-Parkin Cascade

Mechanistically, we linked valinomycin-induced apoptotic response to ubiquitination and degradation of Mcl-1 by Parkin. Mcl-1 is an unstable protein, and its steady-state levels are regulated by several ubiquitin E3 ligases, including Mule [34], SCF^{Fbw7} [35], and SCF^{TrCP} [36]. Here, we provide an example of a signal-regulated Mcl-1 E3 ligase in Parkin. Using a reconstituted in vitro system, we demonstrated that two PINK1-dependent phosphorylation events drive amplification of its autoubiquitination and transubiquitination activity. PINK1 directly phosphorylates Ser65 of Parkin in the Ubl domain and ubiquitin at Ser65. This sets off an autocatalytic cycle for activating Parkin autoubiquitination and transubiquitination of Mcl-1. While we still do not know precisely how Ser65 phosphorylation enables Parkin to adopt an active conformation, we can speculate that phosphorylation in Ubl domain of Parkin may unmask the E2 docking site [23]. It is a mystery why phosphorylated ubiquitin can promote its activity. In essence, Ser65-phosphorylated ubiquitin could be derived from phosphorylation of autoubiquitinated Parkin by PINK1 or conjugation of free ubiquitin phosphorylated by PINK1 or both. Future experiments are needed to determine to what degree ubiquitin is phosphorylated in cells upon PINK1 activation. We show that a Parkin mutant defective in PINK1 phosphorylation can stimulate wild-type Parkin E3 activity in *trans*. This result suggests that Parkin is a preferred substrate for itself and that a small fraction of Parkin phosphorylation by PINK1 can trigger nonlinear amplification of E3 ligase activity. The positive feedback generated by Parkin autoubiquitination and autocatalysis is most likely an underlying mechanism for irreversible cell fate determination. This model provides one explanation of why wild-type Parkin can rescue the defects of Parkin Ser65 mutant and robust Parkin accumulation on mitochondria. It will be interesting to determine whether this mechanism can operate locally in a spatial constrained manner.

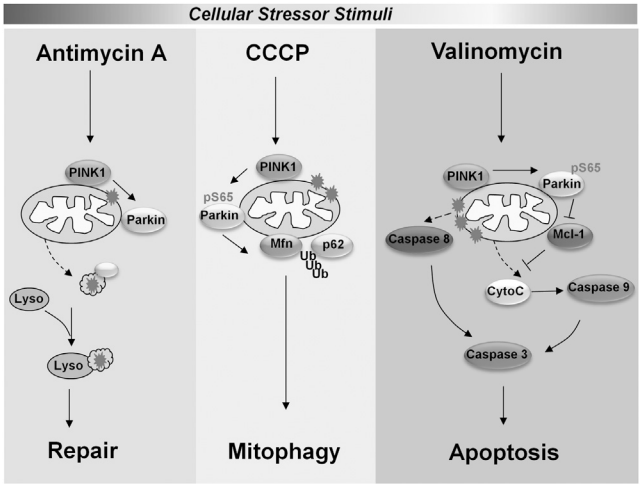

Figure 7. Model Depicting the Tandem Action of PINK1-Parkin as a Damage-Gated Molecular Switch for Cell Fate Specification

Experimental Procedures

Cell Culture, Constructs, and Antibodies

The source of cell lines, recombinant DNA constructs, and antibodies are listed in Supplemental Experimental Procedures.

In Vitro Kinase Assay

Recombinant wild-type and D359A (kinase-dead) in the background of MBP-TcPINK1 and the substrate His_6-Sumo-Parkin (1–108) were purified, and the kinase reactions were performed as described [11].

In Vitro Ubiquitination Assay

Purification of ubiquitin E1, E2 (UbcH7), and reagents for the in vitro ubiquitination assay was described previously [37]. Wild-type or mutant Parkin proteins were purified from *Escherichia coli* as described previously [23]. Human Mcl-1 (1–327 aa) was subcloned in pET15b and was purified by Ni-NTA affinity chromatography. The ubiquitination assays were performed by incubation of 1 μM His_6-Mcl-1 with 0.5 μM E1, 5 μM UbcH7 (E2), 0.7 μM rParkin E3 complex, 20 μM ubiquitin (Sigma), and 1 μl 20 × energy regeneration system (10 mM ATP, 20 mM HEPES [pH 7.4], 10 mM MgOAc, 300 mM creatine phosphate, and 0.5 mg/ml creatine phosphokinase) in a final volume of 20 μl. The reactions were incubated at 37°C for the indicated time, terminated by boiling in 2× SDS protein sample buffer, and analyzed by SDS-PAGE and immunoblotting with the indicated antibodies.

Cell Death Assays

Three independent cell death assays were used. Detailed methods of RFP-Smac release, NucView caspase-3 biosensor, Hoechst 33258 staining, and live cell imaging are described in the Supplemental Experimental Procedures.

Supplemental Information

Supplemental Information includes Supplemental Experimental Procedures, five figures, and three movies and can be found with this article online at http://dx.doi.org/10.1016/j.cub.2014.07.014.

Author Contributions

C.Z. and X.L. designed the study; C.Z., S.L., Y.P., S.M., and Z.Z. performed experiments; C.Z., S.L., E.B., and X.L. analyzed data; E.G. and J.S. provided PINK1- and Parkin-null cell lines; and C.Z., S.L., and X.L. wrote the manuscript.

Acknowledgments

We thank Kevan Shokat, Stefan Constantinescu, Nick Hertz, and Michael Lazarus for providing critical reagents. We thank Kevin Dean, Yan Qin, Junglim Lee, and Genevieve Park for technical assistance. We also want to thank James Goodrich for critical reading of the manuscript; Natalie Ahn, James Ferrell, Tobias Meyer, Amy Palmer, and members of Liu laboratory for discussion; and Miratul Muqit, Helen Walden, Hiroyuki Miyoshi, Xinde Zheng, Tony Hunter, and Sabrina Spencer for expression vectors. This work was supported by grants from a Butcher Award from the University of Colorado, Cancer League of Colorado, and NIH grant CA107098 to X.L. The ImageXpress MicroXL was supported by NCRR grant number S10 RR026680 from the NIH. This work was also in part sponsored by the U.S. Army Research Office and the Defense Advanced Research Projects Agency and was accomplished under Cooperative Agreement number W911NF-14-2-0019.

Received: June 11, 2014
Revised: July 3, 2014
Accepted: July 4, 2014
Published: July 31, 2014

References

1. Valente, E.M., Abou-Sleiman, P.M., Caputo, V., Muqit, M.M.K., Harvey, K., Gispert, S., Ali, Z., Del Turco, D., Bentivoglio, A.R., Healy, D.G., et al. (2004). Hereditary early-onset Parkinson's disease caused by mutations in PINK1. Science *304*, 1158–1160.
2. Dawson, T.M., and Dawson, V.L. (2010). The role of parkin in familial and sporadic Parkinson's disease. Mov. Disord. *25* (*Suppl 1*), S32–S39.
3. Cookson, M.R. (2005). The biochemistry of Parkinson's disease. Annu. Rev. Biochem. *74*, 29–52.
4. Youle, R.J., and Narendra, D.P. (2011). Mechanisms of mitophagy. Nat. Rev. Mol. Cell Biol. *12*, 9–14.
5. Winklhofer, K.F. (2014). Parkin and mitochondrial quality control: toward assembling the puzzle. Trends Cell Biol. *24*, 332–341.
6. Narendra, D., Walker, J.E., and Youle, R. (2012). Mitochondrial quality control mediated by PINK1 and Parkin: links to parkinsonism. Cold Spring Harb. Perspect. Biol. *4*, a011338.
7. Narendra, D.P., Jin, S.M., Tanaka, A., Suen, D.-F., Gautier, C.A., Shen, J., Cookson, M.R., and Youle, R.J. (2010). PINK1 is selectively stabilized on impaired mitochondria to activate Parkin. PLoS Biol. *8*, e1000298.
8. Zhou, C., Huang, Y., Shao, Y., May, J., Prou, D., Perier, C., Dauer, W., Schon, E.A., and Przedborski, S. (2008). The kinase domain of mitochondrial PINK1 faces the cytoplasm. Proc. Natl. Acad. Sci. USA *105*, 12022–12027.
9. Vives-Bauza, C., Zhou, C., Huang, Y., Cui, M., de Vries, R.L.A., Kim, J., May, J., Tocilescu, M.A., Liu, W., Ko, H.S., et al. (2010). PINK1-dependent recruitment of Parkin to mitochondria in mitophagy. Proc. Natl. Acad. Sci. USA *107*, 378–383.
10. Chen, Y., and Dorn, G.W., 2nd. (2013). PINK1-phosphorylated mitofusin 2 is a Parkin receptor for culling damaged mitochondria. Science *340*, 471–475.
11. Kondapalli, C., Kazlauskaite, A., Zhang, N., Woodroof, H.I., Campbell, D.G., Gourlay, R., Burchell, L., Walden, H., Macartney, T.J., Deak, M., et al. (2012). PINK1 is activated by mitochondrial membrane potential depolarization and stimulates Parkin E3 ligase activity by phosphorylating Serine 65. Open Biol. *2*, 120080.
12. Wang, X., Winter, D., Ashrafi, G., Schlehe, J., Wong, Y.L., Selkoe, D., Rice, S., Steen, J., LaVoie, M.J., and Schwarz, T.L. (2011). PINK1 and Parkin target Miro for phosphorylation and degradation to arrest mitochondrial motility. Cell *147*, 893–906.
13. Matsuda, N., Sato, S., Shiba, K., Okatsu, K., Saisho, K., Gautier, C.A., Sou, Y.S., Saiki, S., Kawajiri, S., Sato, F., et al. (2010). PINK1 stabilized by mitochondrial depolarization recruits Parkin to damaged mitochondria and activates latent Parkin for mitophagy. J. Cell Biol. *189*, 211–221.
14. Geisler, S., Holmström, K.M., Skujat, D., Fiesel, F.C., Rothfuss, O.C., Kahle, P.J., and Springer, W. (2010). PINK1/Parkin-mediated mitophagy is dependent on VDAC1 and p62/SQSTM1. Nat. Cell Biol. *12*, 119–131.
15. Wenzel, D.M., Lissounov, A., Brzovic, P.S., and Klevit, R.E. (2011). UBCH7 reactivity profile reveals parkin and HHARI to be RING/HECT hybrids. Nature *474*, 105–108.
16. Zheng, X., and Hunter, T. (2013). Parkin mitochondrial translocation is achieved through a novel catalytic activity coupled mechanism. Cell Res. *23*, 886–897.

17. Lazarou, M., Narendra, D.P., Jin, S.M., Tekle, E., Banerjee, S., and Youle, R.J. (2013). PINK1 drives Parkin self-association and HECT-like E3 activity upstream of mitochondrial binding. J. Cell Biol. *200*, 163–172.
18. Olzmann, J.A., Li, L., Chudaev, M.V., Chen, J., Perez, F.A., Palmiter, R.D., and Chin, L.S. (2007). Parkin-mediated K63-linked polyubiquitination targets misfolded DJ-1 to aggresomes via binding to HDAC6. J. Cell Biol. *178*, 1025–1038.
19. Tanaka, A., Cleland, M.M., Xu, S., Narendra, D.P., Suen, D.-F., Karbowski, M., and Youle, R.J. (2010). Proteasome and p97 mediate mitophagy and degradation of mitofusins induced by Parkin. J. Cell Biol. *191*, 1367–1380.
20. Wang, H., Song, P., Du, L., Tian, W., Yue, W., Liu, M., Li, D., Wang, B., Zhu, Y., Cao, C., et al. (2011). Parkin ubiquitinates Drp1 for proteasome-dependent degradation: implication of dysregulated mitochondrial dynamics in Parkinson disease. J. Biol. Chem. *286*, 11649–11658.
21. Geisler, S., Holmström, K.M., Treis, A., Skujat, D., Weber, S.S., Fiesel, F.C., Kahle, P.J., and Springer, W. (2010). The PINK1/Parkin-mediated mitophagy is compromised by PD-associated mutations. Autophagy *6*, 871–878.
22. Sarraf, S.A., Raman, M., Guarani-Pereira, V., Sowa, M.E., Huttlin, E.L., Gygi, S.P., and Harper, J.W. (2013). Landscape of the PARKIN-dependent ubiquitylome in response to mitochondrial depolarization. Nature *496*, 372–376.
23. Trempe, J.F., Sauvé, V., Grenier, K., Seirafi, M., Tang, M.Y., Ménade, M., Al-Abdul-Wahid, S., Krett, J., Wong, K., Kozlov, G., et al. (2013). Structure of parkin reveals mechanisms for ubiquitin ligase activation. Science *340*, 1451–1455.
24. McLelland, G.L., Soubannier, V., Chen, C.X., McBride, H.M., and Fon, E.A. (2014). Parkin and PINK1 function in a vesicular trafficking pathway regulating mitochondrial quality control. EMBO J. *33*, 282–295.
25. Müller-Rischart, A.K., Pilsl, A., Beaudette, P., Patra, M., Hadian, K., Funke, M., Peis, R., Deinlein, A., Schweimer, C., Kuhn, P.H., et al. (2013). The E3 ligase parkin maintains mitochondrial integrity by increasing linear ubiquitination of NEMO. Mol. Cell *49*, 908–921.
26. Narendra, D., Tanaka, A., Suen, D.-F., and Youle, R.J. (2008). Parkin is recruited selectively to impaired mitochondria and promotes their autophagy. J. Cell Biol. *183*, 795–803.
27. Gautier, C.A., Kitada, T., and Shen, J. (2008). Loss of PINK1 causes mitochondrial functional defects and increased sensitivity to oxidative stress. Proc. Natl. Acad. Sci. USA *105*, 11364–11369.
28. Woodroof, H.I., Pogson, J.H., Begley, M., Cantley, L.C., Deak, M., Campbell, D.G., van Aalten, D.M., Whitworth, A.J., Alessi, D.R., and Muqit, M.M. (2011). Discovery of catalytically active orthologues of the Parkinson's disease kinase PINK1: analysis of substrate specificity and impact of mutations. Open Biol. *1*, 110012.
29. Arena, G., Gelmetti, V., Torosantucci, L., Vignone, D., Lamorte, G., De Rosa, P., Cilia, E., Jonas, E.A., and Valente, E.M. (2013). PINK1 protects against cell death induced by mitochondrial depolarization, by phosphorylating Bcl-xL and impairing its pro-apoptotic cleavage. Cell Death Differ. *20*, 920–930.
30. Hertz, N.T., Berthet, A., Sos, M.L., Thorn, K.S., Burlingame, A.L., Nakamura, K., and Shokat, K.M. (2013). A neo-substrate that amplifies catalytic activity of parkinson's-disease-related kinase PINK1. Cell *154*, 737–747.
31. Klinkenberg, M., Thurow, N., Gispert, S., Ricciardi, F., Eich, F., Prehn, J.H.M., Auburger, G., and Kögel, D. (2010). Enhanced vulnerability of PARK6 patient skin fibroblasts to apoptosis induced by proteasomal stress. Neuroscience *166*, 422–434.
32. Haque, M.E., Thomas, K.J., D'Souza, C., Callaghan, S., Kitada, T., Slack, R.S., Fraser, P., Cookson, M.R., Tandon, A., and Park, D.S. (2008). Cytoplasmic Pink1 activity protects neurons from dopaminergic neurotoxin MPTP. Proc. Natl. Acad. Sci. USA *105*, 1716–1721.
33. Codogno, P., and Meijer, A.J. (2005). Autophagy and signaling: their role in cell survival and cell death. Cell Death Differ. *12* (*Suppl 2*), 1509–1518.
34. Zhong, Q., Gao, W., Du, F., and Wang, X. (2005). Mule/ARF-BP1, a BH3-only E3 ubiquitin ligase, catalyzes the polyubiquitination of Mcl-1 and regulates apoptosis. Cell *121*, 1085–1095.
35. Inuzuka, H., Shaik, S., Onoyama, I., Gao, D., Tseng, A., Maser, R.S., Zhai, B., Wan, L., Gutierrez, A., Lau, A.W., et al. (2011). SCF(FBW7) regulates cellular apoptosis by targeting MCL1 for ubiquitylation and destruction. Nature *471*, 104–109.
36. Ding, Q., He, X., Hsu, J.M., Xia, W., Chen, C.T., Li, L.Y., Lee, D.F., Liu, J.C., Zhong, Q., Wang, X., and Hung, M.C. (2007). Degradation of Mcl-1 by beta-TrCP mediates glycogen synthase kinase 3-induced tumor suppression and chemosensitization. Mol. Cell. Biol. *27*, 4006–4017.
37. Ungermannova, D., Gao, Y., and Liu, X. (2005). Ubiquitination of p27Kip1 requires physical interaction with cyclin E and probable phosphate recognition by SKP2. J. Biol. Chem. *280*, 30301–30309.

Note Added in Proof

While this manuscript was under review, the following publications independently reported the finding of phosphorylation of ubiquitin and Parkin by PINK1:

Kane, L.A., Lazarou, M., Fogel, A.I., Li, Y., Yamano, K., Sarraf, S.A., Banerjee, S., and Youle, R.J. (2014). PINK1 phosphorylates ubiquitin to activate Parkin E3 ubiquitin ligase activity. J. Cell Biol. *205*, 143–153.

Kazlauskaite, A., Kelly, V., Johnson, C., Baillie, C., Hastie, C.J., Peggie, M., Macartney, T., Woodroof, H.I., Alessi, D.R., Pedrioli, P.G., et al. (2014). Phosphorylation of Parkin at Serine65 is essential for activation: elaboration of a Miro1 substrate-based assay of Parkin E3 ligase activity. Open Biol. *4*, 130213.

Kazlauskaite, A., Kondapalli, C., Gourlay, R., Campbell, D.G., Ritorto, M.S., Hofmann, K., Alessi, D.R., Knebel, A., Trost, M., and Muqit, M.M. (2014). Parkin is activated by PINK1-dependent phosphorylation of ubiquitin at Ser65. Biochem. J. *460*, 127–139.

Koyano, F., Okatsu, K., Kosako, H., Tamura, Y., Go, E., Kimura, M., Kimura, Y., Tsuchiya, H., Yoshihara, H., Hirokawa, T., et al. (2014). Ubiquitin is phosphorylated by PINK1 to activate parkin. Nature *510*, 162–166.

Current Biology, Volume *24*

Supplemental Information

PINK1 Triggers Autocatalytic Activation of Parkin to Specify Cell Fate Decisions

Conggang Zhang, Schuyler Lee, Yinghua Peng, Eric Bunker, Emilie Giaime, Jie Shen, Zongyao Zhou, and Xuedong Liu

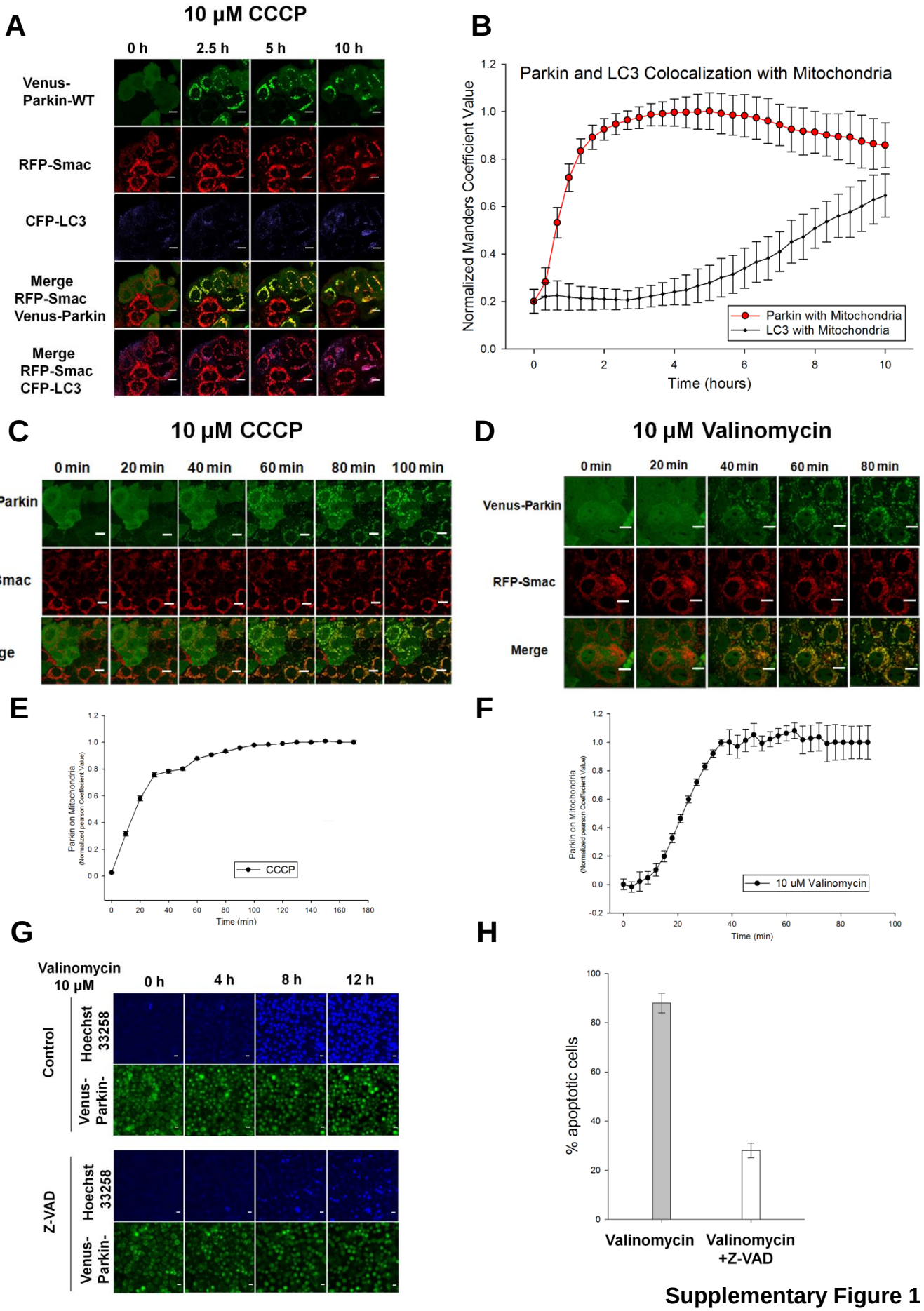

Supplementary Figure 1

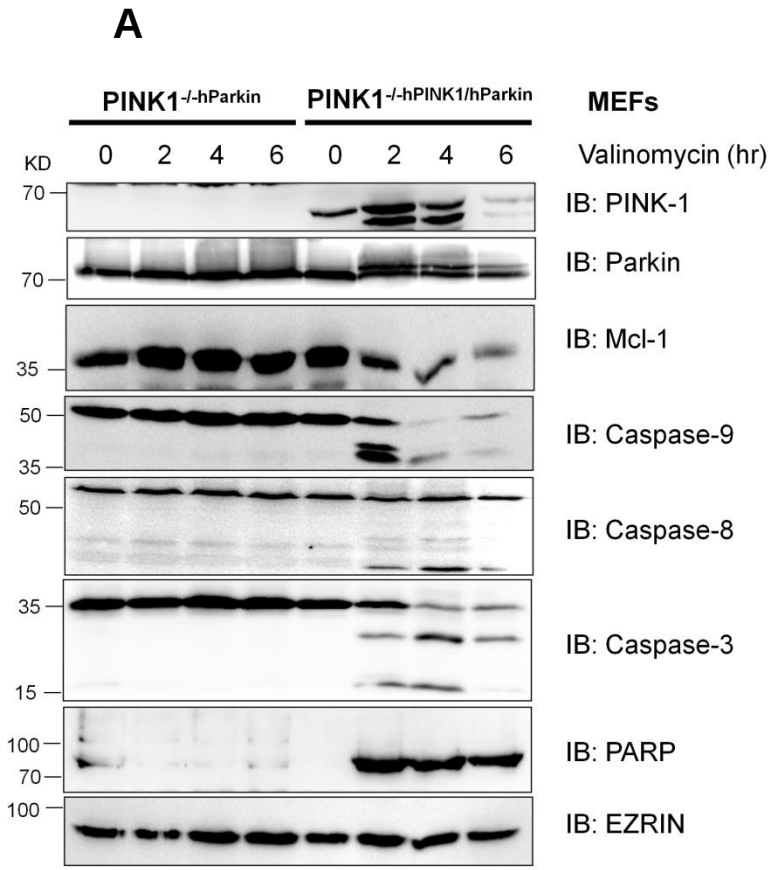

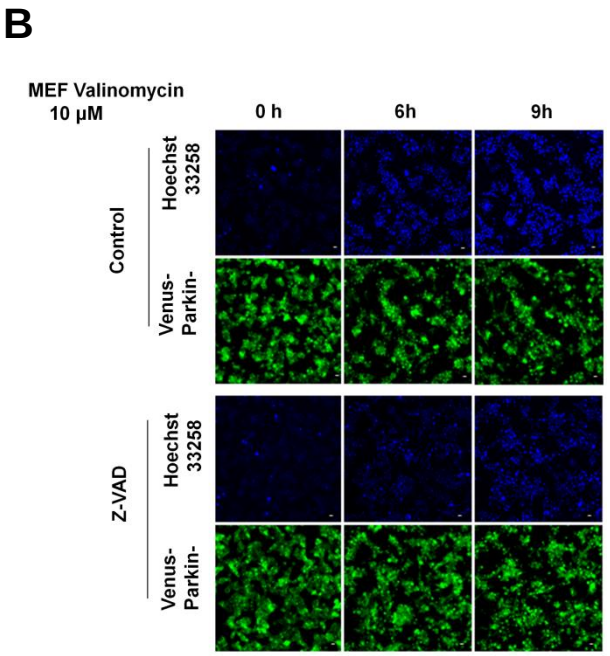

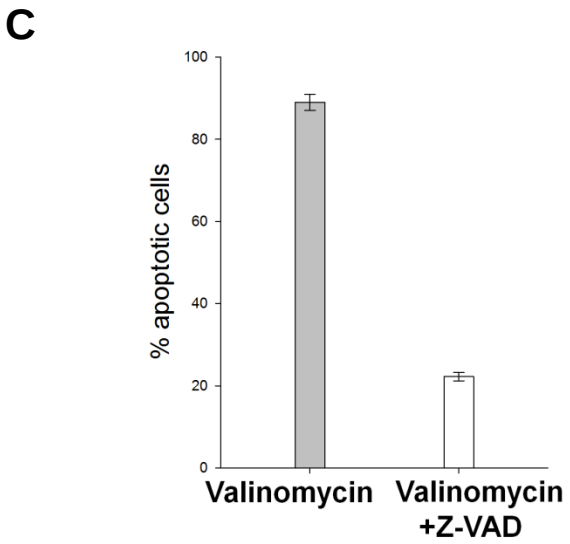

Supplementary Figure 2

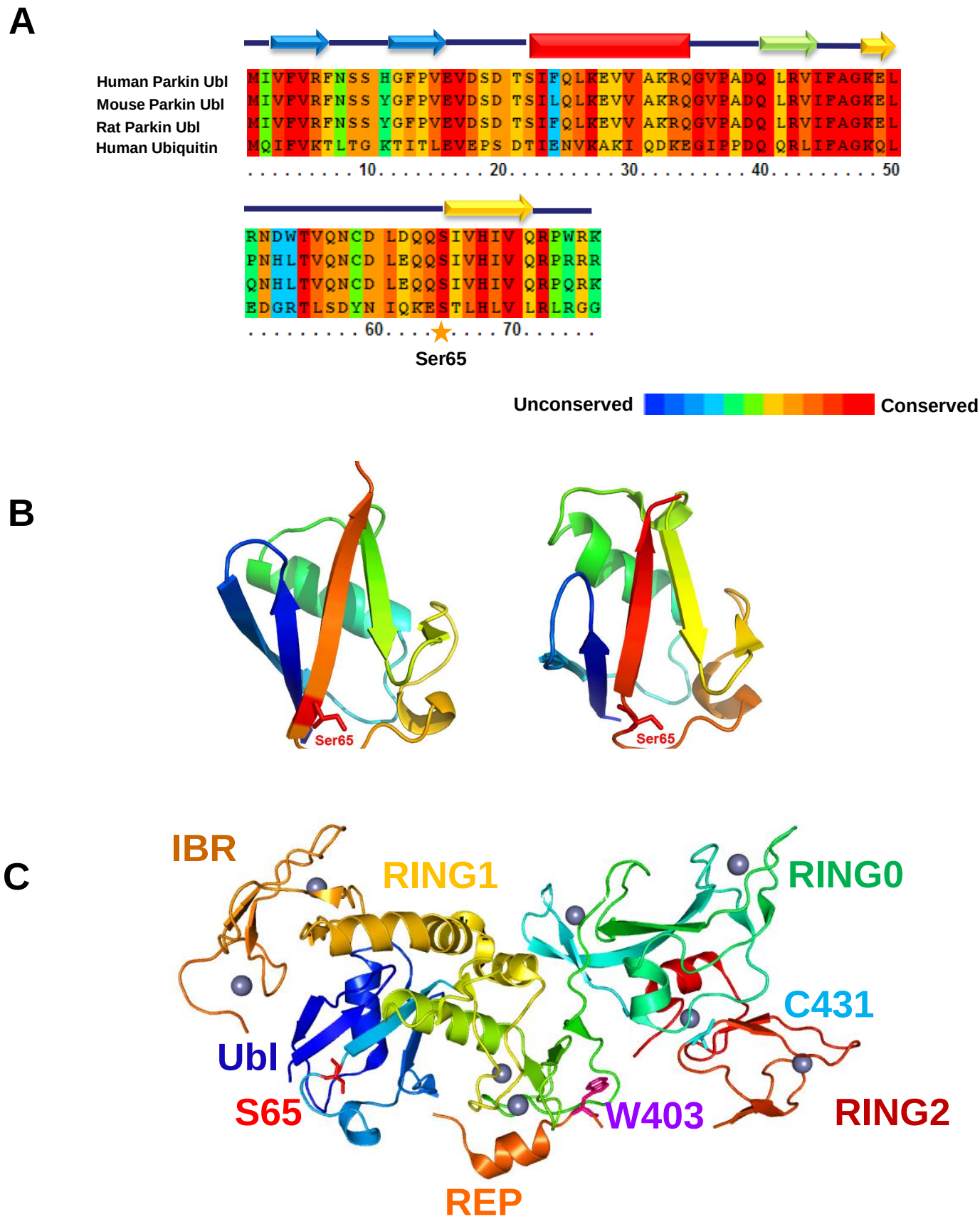

Supplementary Figure 3ABC

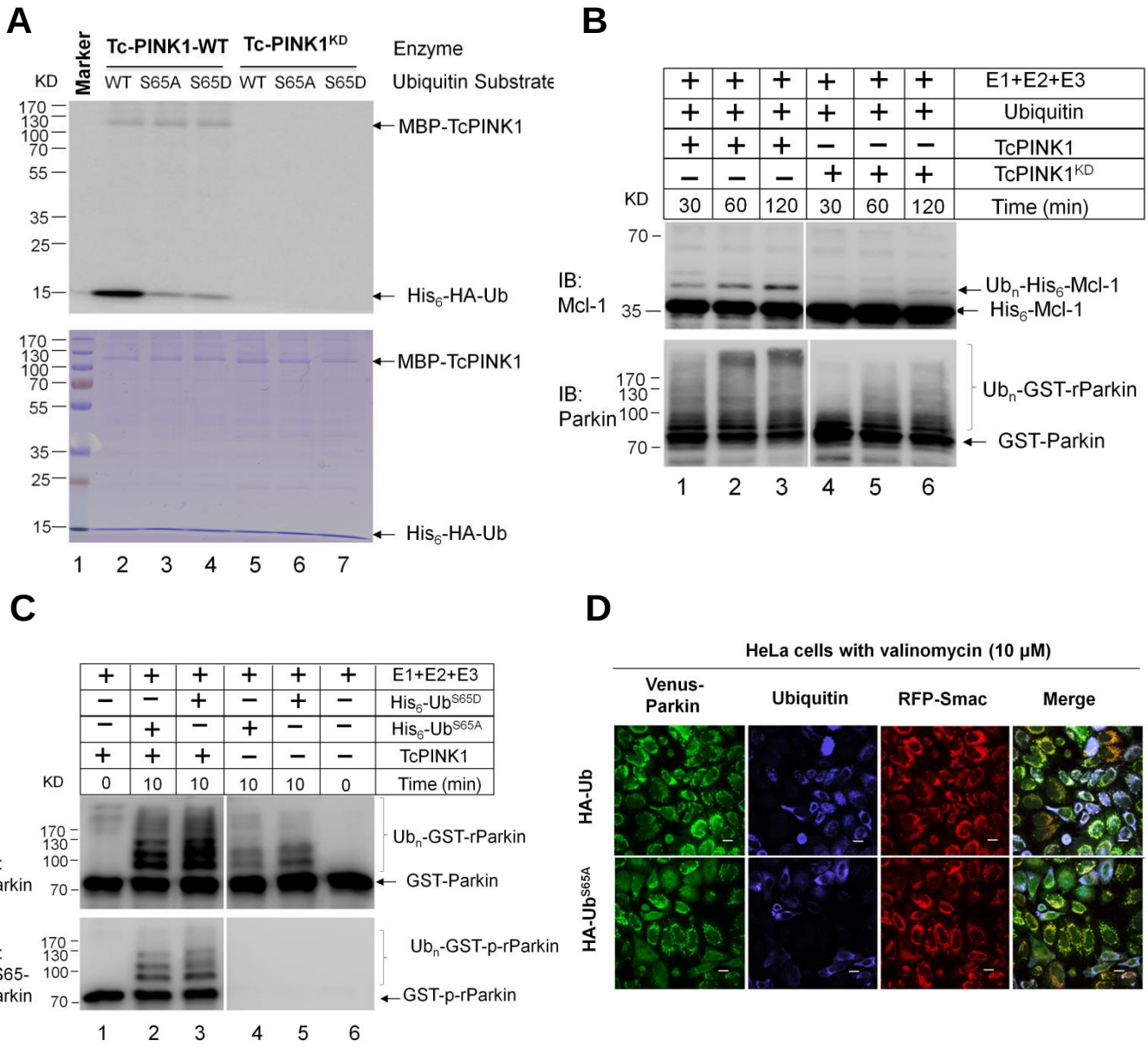

Supplementary Figure 4

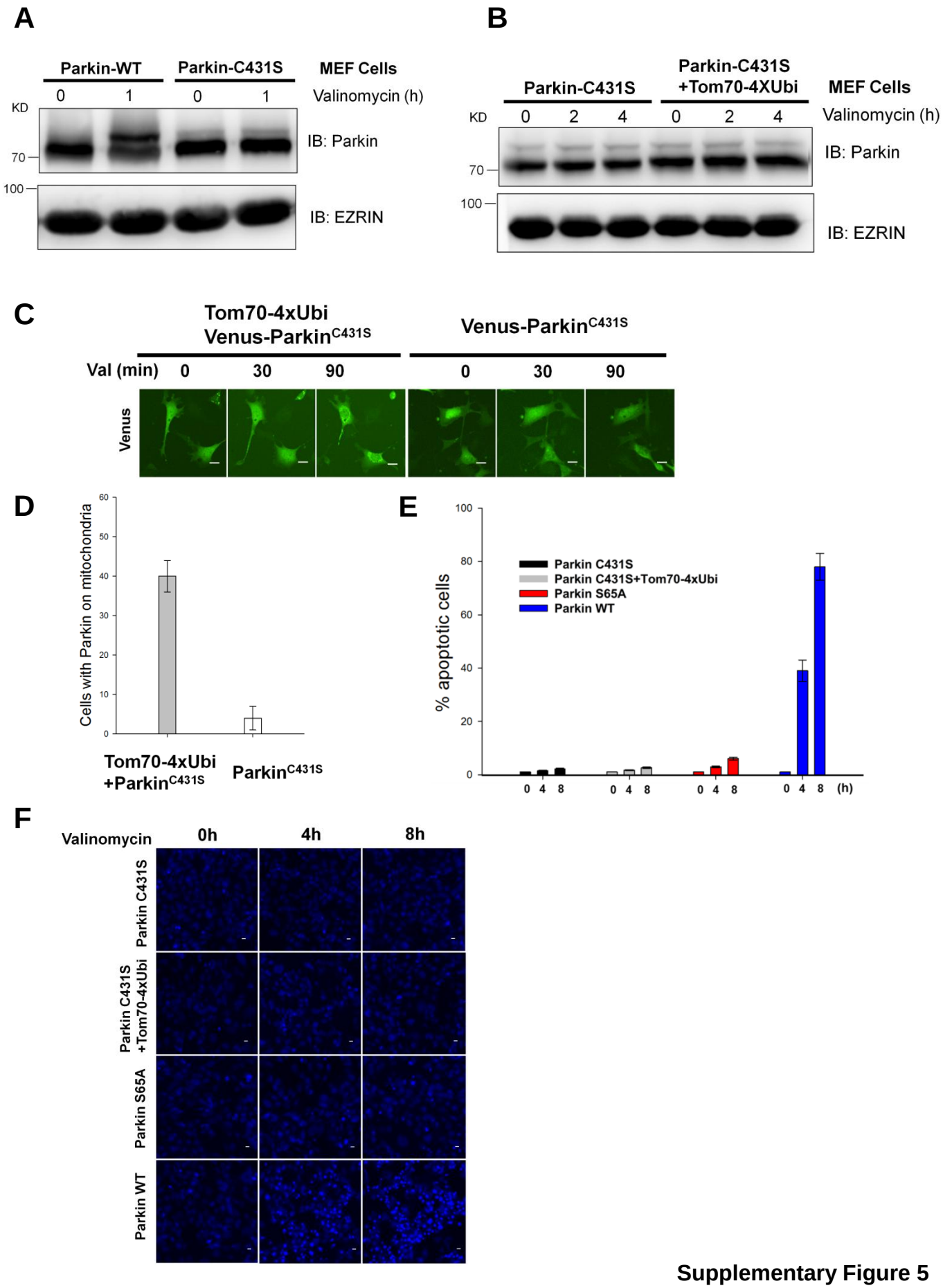

Supplementary Figure 5

Supplementary Figure 1. CCCP and valinomycin elicit different cell fate outcomes in a PINK1/Parkin-dependent manner (related to Figure 1).

(A and B) HeLa cells expressing Venus-Parkin-WT, RFP-Smac and CFP-LC3 were treated with 10μM CCCP in a 10-hour time course. Mitophagy response was visualized with fluorescent microscopy exhibiting translocation of Parkin and LC3 to the mitochondria (A) and quantified by collecting image pairs and analyzed via MATLAB to detect colocalization (B).
(C-F) HeLa cells expressing Venus-Parkin-WT and RFP-Smac were treated with 10μM CCCP in a 100-min time course (C and E) or 10μM Valinomycin in an 80-min time course (D and F). Parkin localization to Mitochondria was visualized with fluorescent microscopy (C and D) and quantified by collecting image pairs and analyzed via MATLAB to detect colocalization (E and F). CCCP and Valinomycin triggered similar phenotypic responses apropos of Parkin localization to mitochondria in HeLa cells.
(G and H) HeLa cells expressing Venus-Parkin-WT and stained with Hoechst 33258 were treated with 10μM Valinomycin in the presence or absence of Z-VAD in a 12-hour time course. Cells were incubated with valinomycin for 1.5h prior to image capture. Apoptotic cell death was visualized with fluorescent microscopy (G) and quantified by counting cells positive for condensed chromatin using MetaXpress as described in Figure 1 (H). Scale bar, 10 μm.

Supplementary Figure 2. Valinomycin induces Parkin-dependent suppression of Mcl-1 and activation of apoptotic initiator caspases in MEF cells (related to Figure 2).

(A) PINK1 null MEF cells were reconstituted by expression of human PINK1 (hPINK1) and human Parkin (hParkin) respectively and subjected to 10μM valinomycin in a 6-hour time course. Pro-apoptotic and anti-apoptotic proteins were monitored by western blotting using antibodies for their respective proteins. Upon valinomycin treatment, cells with restored PINK1-Parkin pathway exhibited a depletion of Mcl-1 levels, activation of Caspase-8 and -9, and cleavage of Caspase-3 and PARP. The corresponding apoptotic response was not detected in PINK1 null cells. (B) and (C) MEF cells expressing Venus-Parkin-WT and stained with Hoeschst 33258 were treated with 10μM valinomycin in the presence or absence of Z-VAD in a 9-hour time course. Cells were incubated with valinomycin for 1h prior to image capture. Apoptotic cell death was visualized with fluorescent microscopy (B) and quantified by scoring the percentage of apoptotic nuclei. Scale bar, 10 μm.

Supplementary Figure 3. Sequence alignment and structural highlights of Parkin and Ubiquitin (related to Figure 4).

(A) PRALINE multiple sequence alignment of Parkin and human ubiquitin. S65 residue in the Ubl domain of Parkin is highlighted with a star. Secondary elements in Ubl domain and ubiquitin are shown above the sequence alignment.
(B) Structure comparison of Ubiquitin and Parkin Ubl domain. Ubiquitin (PDB: 1UBQ) and Parkin (PDB:4K95) structures were displayed using Pymol.
(C) Crystal structure of rParkin (PDB:4K95). Key residues and the relevant functional domains are indicated.

Supplementary Figure 4. Phosphorylation of ubiquitin at Ser^{65} by PINK1 promotes Parkin activation and mitochondrial recruitment (related to Figure 4).

(A) Phosphorylation of ubiquitin by PINK1 at Ser^{65}. Ubiquitin is a novel substrate of PINK1 and Ser^{65} residue of ubiquitin is essential for phosphorylation by TcPINK1. (B) Ubiquitin phosphorylation enhances Parkin E3 ligase activity. Ubiquitin was incubated with TcPINK1 or kinase dead TcPINK1 for 60 min to allow phosphorylation to occur. Phosphorylated and unphosphorylated ubiquitin were used as input for Parkin auto- and trans-ubiquitination reactions *in vitro*. The enhanced auto-ubiquitination and trans-ubiquitination activity
were measured by immunoblotting with indicated antibodies and early appearance of ubiquitylated species. (C) The effect of 5 μM phospho-mimetic ubiquitin (Ub^{S65D}) and nonphosphorylatable ubiquitin (Ser^{S65A}) on Parkin auto-ubiquitination. Either phosphorylated rParkin or nonphosphorylated rParkin were used. Phosphorylated rParkin was made by incubating rParkin with TcPINK1 for 60 min prior to the ubiquitination reaction. Since auto-ubiquitination has a fast kinetics, the reaction was terminated at 10 min. (D) and (E) Expression of nonphosphorylatable ubiquitin ($HA\text{-}Ubiquitin^{S65A}$) suppresses valinomycin induced Parkin mitochondrial recruitment. Scale bar, 10 μm.

Supplementary Figure 5. Requirement of autocatalytic activity of Parkin for valinomycin-induced apoptosis (related to Figure 6).

(A) and (B) Immunoblotting analysis of $PINK1^{-/-}$ $Parkin^{-/-}$ MEF-hPINK1 cells expressing Venus-Parkin or $Venus\text{-}Parkin^{C431S}$ or Venus- $Parkin^{C431S}$ along with Tom70-4xUbi. $Parkin^{C431S}$ is catalytically inactive. (C) and (D) Mitochondrial recruitment of $Venus\text{-}Parkin^{C431S}$ with or without coexpression of Tom70-
4xUbi in response to valinomycin treatment. Scale bar, 10 μm. (E) $PINK1^{-/-}$ $Parkin^{-/-}$ MEF-hPINK1 cells expressing $Venus\text{-}Parkin^{C431S}$, $Venus\text{-}Parkin^{C431S}$ along with Tom70-4xUbi, $Venus\text{-}Parkin^{WT}$ and $mTurquoise\text{-}Parkin^{S65A}$ were treated with valinomycin for indicated time. Apoptotic cell death was quantified by scoring the percentage of apoptotic nuclei. (F) $PINK1^{-/-}$ $Parkin^{-/-}$ MEF-hPINK1 cells expressing $Venus\text{-}Parkin^{C431S}$, $Venus\text{-}Parkin^{C431S}$ along with Tom70-4xUbi, $Venus\text{-}Parkin^{WT}$ and $mTurquoise\text{-}Parkin^{S65A}$ treated with valinomycin for indicated time. Cells were fixed and stained with Hoechst 33258 to obtain 10x images. Scale bar, 10 μm.

Supplemental Experimental Procedures

Constructs. Venus-tagged Parkin constructs were generated by fusion of Parkin wild-type and mutant cDNAs to N-terminal epitope tags using gateway cloning vector pREX-Venus-DEST-IRES-Blasticidin, which is a derivative of a set of retroviral expression vectors described previously [S1]. For generation of PINK1 wild-type and mutant constructs, PINK1 was cloned into CSII-EF-DEST-IRES- Hygromycin lentiviral vectors (gift of Dr. Hiroyuki Miyoshi). The pMSCV-CMV-puro-IMS-RFP, a kind gift from Dr. Sabrina Spencer (Stanford University) was used as mitochondria marker as described previously [S2]. MBP-TcPINK1 and His_6-Sumo-Parkin were gifts of Dr. Miratul Muqit (University of Dundee) and Dr. Helen Walden (Cancer Research UK) respectively. pRK5-HA-Ubiquitin (17608), pGEX-Parkin (45969), GST-Parkin W403A (45974) and GST-Parkin C431SW403A (45977), pBabe-HA-mMcl-1 (25385) and pBabe-Flag-hMcl-1 (25371) were purchased from Addgene. GST-Parkin S65A, pRK5-HA-Ubiquitin S65A and Ubiquitin S65D were constructed by Quikchange mutagenesis (Agilent).

Cell culture, transfection and reagent treatment. HEK293T cells were obtained from the ATCC (American Type Culture Collection). HeLa was a gift of Sabrina Spencer [S2]. Parkin and PINK1 wild type and null MEF cells were described previously [S3]. HeLa and HEK293T cells were maintained in Dulbecco's Modified Eagle's Medium (DMEM) supplemented with 10% fetal calf serum (Invitrogen), penicillin, streptomycin (100 IU/ml and 100 mg/ml, respectively), and L-Glutamine. MEFs were grown in Dulbecco's Modified Eagle's Medium containing 10% fetal bovine serum, penicillin (100 U/mL), streptomycin (100 U/mL), 1 mM l-glutamine, 1mM Na-pyruvate, and 1× nonessential amino acids. All the stable cell lines made by lentivirus and retrovirus packaging were selected with 100 μg/ml hygromycin (Alexis Biochemicals), 5 μg/ml blasticidin (Invitrogen), or 2 μg/ml puromycin (Sigma) based on the selection markers. Mitochondrial membrane potential was dissipated with 10 μM (for HeLa) or 10-20 μM (for MEF) carbonyl cyanide m-chlorophenyl hydrazone (CCCP, Sigma-Aldrich) and 10 μM Valinomycin (Cayman).

Antibodies. Antibodies used in this study for western blot (WB) were: mouse anti-Parkin (1:5000; clone PRK8, Sigma-Aldrich), rabbit anti-PINK1 (1:1000; BC100-494, Novus Biologicals), mouse anti-EZRIN (1:5000, Sigma-Aldrich). Anti-caspase-3, 8, 9, PARP, Mcl-1, Bcl2, Bcl-xL antibodies were purchased from Cell Signaling Technology. Parkin phospho-Ser65 antibody is a gift of Kevan Shokat [S4].

Cell death assays. Three independent cell death assays were used. For the HeLa cells stably expressing RFP-Smac, cell death was monitored by quantifying RFP-Smac release from mitochondria as described previously [S2,S5]. More than 500 cells per condition were inspected. Live cell imaging of cell apoptosis in MEF cells were performed using NucView™488 (Biotium). MEFs were grown on 96-well plates overnight to reach a density of 4×10^4 cells/well. 4 μM NucView caspase-3 biosensor was added. HCS microscope ImageXpress (Molecular Devices) was employed to collect images at indicated time. Typically 10x objective was used for cell death analysis and four independent sites per well of a 96 well plate were imaged. At least 1000 cells per well were examined and quantified. For quantitation of caspase-3 activation in MEF cells, 2 μg/ml of Hoechst dye was included in the media to obtain the total number of nuclei in the field of view. The number of NucView™488 positive cells relative to the total number of nuclei was determined and plotted.

Apoptotic cell death was also visualized and scored by staining with Hoechst 33258 which enters all cells regardless cell health. The average intensity of DNA labeling significantly increases in apoptotic cells as nuclei condense during apoptosis. Quantitation of cell death was performed using automated high content analysis cell heath application module in MetaXpress software (Molecular Devices).

Live cell imaging and immunofluorescence microscopy. To obtain high throughput images and movies, cells were grown on Costar 96-well plates. Molecular Devices ImageXpress XL is used to screen the plates and collect data. Live cell imaging was collected for 1-5 h (for mitochondrial localization of Parkin) and 6-20 h (for apoptosis and mitophagy) for HeLa and MEF cells. To get high resolution images and movies for Parkin mitophagy, cells were growing on 4 well glass bottom chamber (Lab-Tek). Confocal images were acquired on a Nikon A1R Confocal and TIRF using a 100X (NA 1.45) objective. For immunofluorescence microscopy, cells were fixed with 4% paraformaldehyde. Immunofluorescence microscopy was performed as described previously [S6].

Statistical analysis. The Parkin localization in mitochondria and HeLa cells apoptosis were assessed by visually scoring more than 500 cells per stable cell line, in at least three independent experiments. For quantification of MEFs apoptosis, more than 5000 cells were quantified per condition using MetaXpress Multiwavelength Cell Scoring Application Module (Molecular Devices). Standard deviations were calculated from at least three sets of data. The p values are determined using SigmaPlot.

Supplemental References

S1. Liu, X., Constantinescu, S.N., Sun, Y., Bogan, J.S., Hirsch, D., Weinberg, R.A., and Lodish, H.F. (2000). Generation of mammalian cells stably expressing multiple genes at predetermined levels. Anal Biochem *280*, 20-28.

S2. Spencer, S.L., Gaudet, S., Albeck, J.G., Burke, J.M., and Sorger, P.K. (2009). Non-genetic origins of cell-to-cell variability in TRAIL-induced apoptosis. Nature *459*, 428-432.

S3. Gautier, C.A., Kitada, T., and Shen, J. (2008). Loss of PINK1 causes mitochondrial functional defects and increased sensitivity to oxidative stress. Proc Natl Acad Sci U S A *105*, 11364-11369.

S4. Hertz, N.T., Berthet, A., Sos, M.L., Thorn, K.S., Burlingame, A.L., Nakamura, K., and Shokat, K.M. (2013). A Neo-Substrate that Amplifies Catalytic Activity of Parkinson's-Disease-Related Kinase PINK1. Cell *154*, 737-747.

S5. Spencer, S.L., and Sorger, P.K. (2011). Measuring and modeling apoptosis in single cells. Cell *144*, 926-939.

S6. Liu, X., Sun, Y., Ehrlich, M., Lu, T., Kloog, Y., Weinberg, R.A., Lodish, H.F., and Henis, Y.I. (2000). Disruption of TGF-beta growth inhibition by oncogenic ras is linked to p27Kip1 mislocalization. Oncogene *19*, 5926-5935.